U.S. DEPARTMENT OF COMMERCE/Environmental Science Services Administration

Technical Report

ESSA RESEARCH LABORATORIES

ERL 69–WPL 4

A Survey of Microwave Fading Mechanisms Remedies and Applications

MARCH 1968

Boulder, Colorado

ESSA RESEARCH LABORATORIES

The mission of the Research Laboratories is to study the oceans, inland waters, the lower and upper atmosphere, the space environment, and the earth, in search of the understanding needed to provide more useful services in improving man's prospects for survival as influenced by the physical environment. Laboratories contributing to these studies are:

Earth Sciences Laboratories: Geomagnetism, seismology, geodesy, and related earth sciences; earthquake processes, internal structure and accurate figure of the Earth, and distribution of the Earth's mass.

Atlantic Oceanographic Laboratories and Pacific Oceanographic Laboratories: Oceanography, with emphasis on ocean basins and borders, and oceanic processes; sea-air interactions; and land-sea interactions. (Miami, Florida)

Atmospheric Physics and Chemistry Laboratory: Cloud physics and precipitation; chemical composition and nucleating substances in the lower atmosphere; and laboratory and field experiments toward developing feasible methods of weather modification.

Air Resources Laboratories: Diffusion, transport, and dissipation of atmospheric contaminants; development of methods for prediction and control of atmospheric pollution. (Silver Spring, Maryland)

Geophysical Fluid Dynamics Laboratory: Dynamics and physics of geophysical fluid systems; development of a theoretical basis, through mathematical modeling and computer simulation, for the behavior and properties of the atmosphere and the oceans. (Washington, D. C.)

National Hurricane Research Laboratory: Hurricanes and other tropical weather phenomena by observational, analytical, and theoretical means; hurricane modification experiments to improve understanding of tropical storms and prediction of their movement and severity. (Miami, Florida)

National Severe Storms Laboratory: Tornadoes, squall lines, thunderstorms, and other severe local convective phenomena toward achieving improved methods of forecasting, detecting, and providing advance warnings. (Norman, Oklahoma)

Space Disturbances Laboratory: Nature, behavior, and mechanisms of space disturbances; development and use of techniques for continuous monitoring and early detection and reporting of important disturbances.

Aeronomy Laboratory: Theoretical, laboratory, rocket, and satellite studies of the physical and chemical processes controlling the ionosphere and exosphere of the earth and other planets.

Wave Propagation Laboratory: Development of new methods for remote sensing of the geophysical environment; special emphasis on propagation of sound waves, and electromagnetic waves at millimeter, infrared, and optical frequencies.

Institute for Telecommunication Sciences: Central federal agency for research and services in propagation of radio waves, radio properties of the earth and its atmosphere, nature of radio noise and interference, information transmission and antennas, and methods for the more effective use of the radio spectrum for telecommunications.

Research Flight Facility: Outfits and operates aircraft specially instrumented for research; and meets needs of ESSA and other groups for environmental measurements for aircraft. (Miami, Florida)

ENVIRONMENTAL SCIENCE SERVICES ADMINISTRATION

BOULDER, COLORADO

U. S. DEPARTMENT OF COMMERCE
C. R. Smith, Secretary

ENVIRONMENTAL SCIENCE SERVICES ADMINISTRATION
Robert M. White, Administrator

ESSA RESEARCH LABORATORIES
George S. Benton, Director

ESSA TECHNICAL REPORT ERL 69-WPL 4

A Survey of Microwave Fading Mechanisms Remedies and Applications

H. T. DOUGHERTY

WAVE PROPAGATION LABORATORIES
BOULDER, COLORADO
March 1968

For sale by the Superintendent of Documents, U.S. Government Printing Office, Washington, D.C. 20402
Price 50 cents.

TABLE OF CONTENTS

LIST OF FIGURES

A SURVEY OF MICROWAVE FADING MECHANISMS AND REMEDIES

H. T. Dougherty

After a brief description of the significance of the radio refractive index and its variation in the lower troposphere, a catalog of fading mechanisms is presented. Attention is directed to the supporting refractive index structure, the characteristics of the fading signal, and the available remedies. The phenomena of multipath fading are described, and the theoretical amplitude distributions are presented. Diversity reception (frequency or space) is outlined for reducing the fading due to multipath. Specific expressions are given for determining the frequency or space separations.

Successful remedies for microwave fading that are keyed to specific fading mechanisms also constitute a means of measuring the characteristics of the prevailing meteorological conditions. Specific expressions are given to accomplish this for the multipath and diffraction fading mechanisms.

1. INTRODUCTION

It is well known that changes in the radio refractive index structure along nominally line-of-sight propagation paths cause variation of the received signal level. For most line-of-sight communication systems most of the time, this signal variation is not serious. The serious variation, fading, is generally limited to systems operating in the upper UHF and the SHF frequency bands in certain geographical locations and at particular times of the day and year. A wealth of experience pertinent to this fading has been provided by the efforts of experimentalists and system operators over the last two decades.

Much of the experimental data has been described by Beckmann and Spizzichino (1963) and abstracts of many of the published reports are available (Dougherty, 1964). This experience must now be made available in a form readily assimilated by the systems engineer and future investigators. This requires a proper cataloging of fading in terms of the prevailing propagation mechanisms, the associated meteorological and terrain conditions, the observable fading characteristics, and the advantages and limitations of the available remedies.

This is the first report of a study undertaken at the ESSA Research Laboratories. The purpose is to determine a proper cataloging, with two applications in mind. First, the cataloging should permit the systems engineer to diagnose a fading situation and select the most economic and effective remedy--at least to the extent permitted by the experience accumulated to date. Second, the cataloging should permit the design of critical experiments to test and to extend our understanding of fading phenomena. Initially, the study involves the fields of wave propagation, meteorology and statistics, but must eventually involve the fields of modulation systems and techniques. The latter is necessary because fading involves not just variations of signal amplitude, but also of the phase, angle of arrival, and polarization of the received signal.

The most basic definitions of fading are in terms of the propagation mechanisms involved: refraction, reflection, diffraction, scattering, focusing, attenuation, etc., as well as the guiding of radio waves. These are basic because they determine the statistical behavior with time of the measurable field parameters (amplitude, phase, and polarization) and the frequency and spatial selectivity of the fading. These mechanisms are also basic because the most efficient fading remedies are keyed to recognizing the causative mechanism. They are encountered,

however, only in the presence of certain associated conditions classified as meteorological situations and terrain geometry. These conditions are usually related in severe fading situations, and, in most cases, sufficiently understood to be categorized in terms of why, where, and when. Although the predictability of these associated conditions is not suitable for inclusion in the formal telecommunication system design procedures, it can be described so that the systems engineer can avoid the more "obvious" causes of fading in the course of his site survey.

Because some systems engineers may not be familiar with the variation of radio refractivity near the earth's surface, this report will first attempt to summarize (section 2) what is known about certain aspects of the radio refractive index (its structure and variation) that are significant for microwave fading. In section 3, the fading mechanisms are classified and illustrated in terms of the supporting refractive index structure and the terrain geometry. The fading characteristics are described, qualitatively, and the available remedies are discussed in general. Section 4 presents the families of theoretical distributions, i.e., the amplitude fading distributions that would be expected for multipath fading mechanisms. The multipath fading mechanisms are discussed further in section 5, and the reduction of their effects, by diversity system design, is detailed. Section 6 treats the use of multipath and diffraction fading remedies as techniques to measure the characteristics of the supporting meteorological and terrain conditions. Section 7 briefly summarizes the regions in which further study is particularly needed.

2. REFRACTIVE INDEX GRADIENTS

This section briefly describes some of the available information about the refractive index structure near the earth's surface that is significant in connection with microwave fading mechanisms.

The average bending of an electromagnetic wave propagated through the troposphere may usually be represented by ray theory (Bean, 1964; Born and Wolf, 1964; Bean and Dutton, 1966) in terms of a radius of ray curvature related to the average gradient of refractive index (Schelleng, Burrows and Ferrell, 1933; Millington, 1946, and 1957; Dutton and Thayer, 1961; and Beckmann, 1962). If we assume that the refractive index n of the air varies linearly with the height h for the first few tenths of a kilometer above the earth's surface and does not vary in a horizontal direction, then the radius of curvature r of the radio ray relative to the radius of the earth, $r_0 \approx 6370$ km, may be expressed in terms of the gradient, $\Delta n/\Delta h$, by:

$$r/r_0 = k \approx \left[1 + r_0 \frac{\Delta n}{\Delta h} \right]^{-1} . \qquad (1)$$

The parameter k is sometimes known as the effective earth-radius factor. The gradient is usually expressed in terms of the refractivity, $N = (n-1)\,10^6$, so that

$$\frac{\Delta n}{\Delta h} = \frac{\Delta N}{\Delta H}\ 10^{-6} \text{ N units/km} , \qquad (2)$$

and

$$k \approx \left[1 + \left(\frac{\Delta N}{\Delta h}\right) / 157 \right]^{-1} . \qquad (3)$$

Several values of k and $\Delta N/\Delta h$ are listed in figure 1, where the corresponding ray paths are illustrated. The vertical scale of figure 1 is exaggerated, relative to the horizontal scale, to make the differences in curvature noticeable.

For $0 < k < 1.0$, encountered for positive gradients (subrefractive conditions), the ray curves away from the earth so that the ray joining two terminals passes close to the earth. The ray may even be interrupted by the surface ($k = 0.33$ in fig. 1) so that the receiving terminal is beyond radio line of sight. For the commonly encountered situations $-157 \leq \Delta N/\Delta h \leq 0$ where $\infty \geq k \geq 1.0$, the rays are bent toward the earth's surface. At the critical value $\Delta N/\Delta h = -157$ N units/km, $|k| = \infty$ and the curvature of the ray path is equal to the curvature of the earth; the rays follow straight paths relative to the earth's surface. For $\Delta N/\Delta h < -157$, the situation is superrefractive and the value of k, given by (3), is negative. For negative values (Hufford, 1967), the ray paths are bent sufficiently toward the earth's surface so that trapping of the radio rays is possible. Because of that possibility, $\Delta N/\Delta h < -157$ is commonly referred to as a trapping or ducting condition. The relation between the values of k and $\Delta N/\Delta h$, discussed above and given by (3), is plotted in figure 2.

To illustrate that the range of conditions shown in figure 1 is realistic, a distribution of average gradients for Cape Kennedy, Florida, is presented in figure 3. The distribution was determined from February, May, August, and November data selected from a 7-year period. This figure is based on data from the World Radio Refractive Index Data Center at the Environmental Science Services Administration, Boulder, Colorado. Preliminary investigations for other locations throughout the world indicate that figure 3 at least exemplifies maritime or coastal locations with relatively smooth terrain. Much of the

THE BENDING OF RADIO RAYS FOR LINEAR GRADIENTS

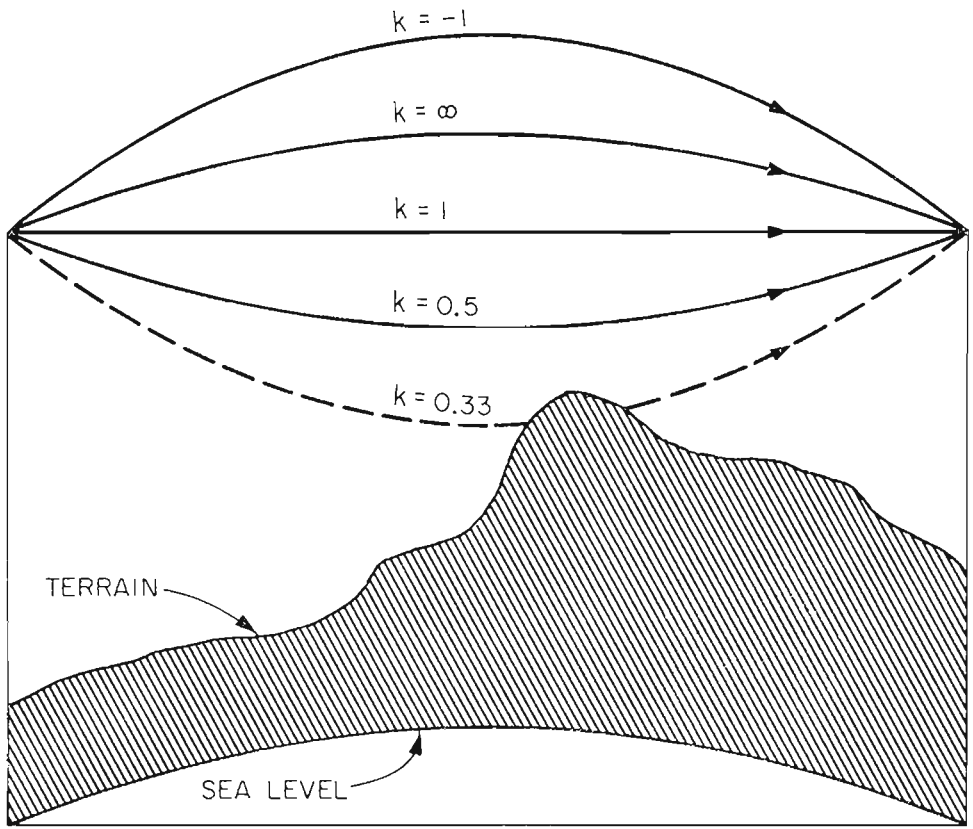

$*\frac{\Delta N}{\Delta h}$	k
314	0.33
157	0.5
0	1.0
-157	∞
-314	-1.0

* N UNITS/km

Figure 1

EFFECTIVE EARTH RADIUS FACTOR VERSUS THE LINEAR REFRACTIVE INDEX GRADIENT

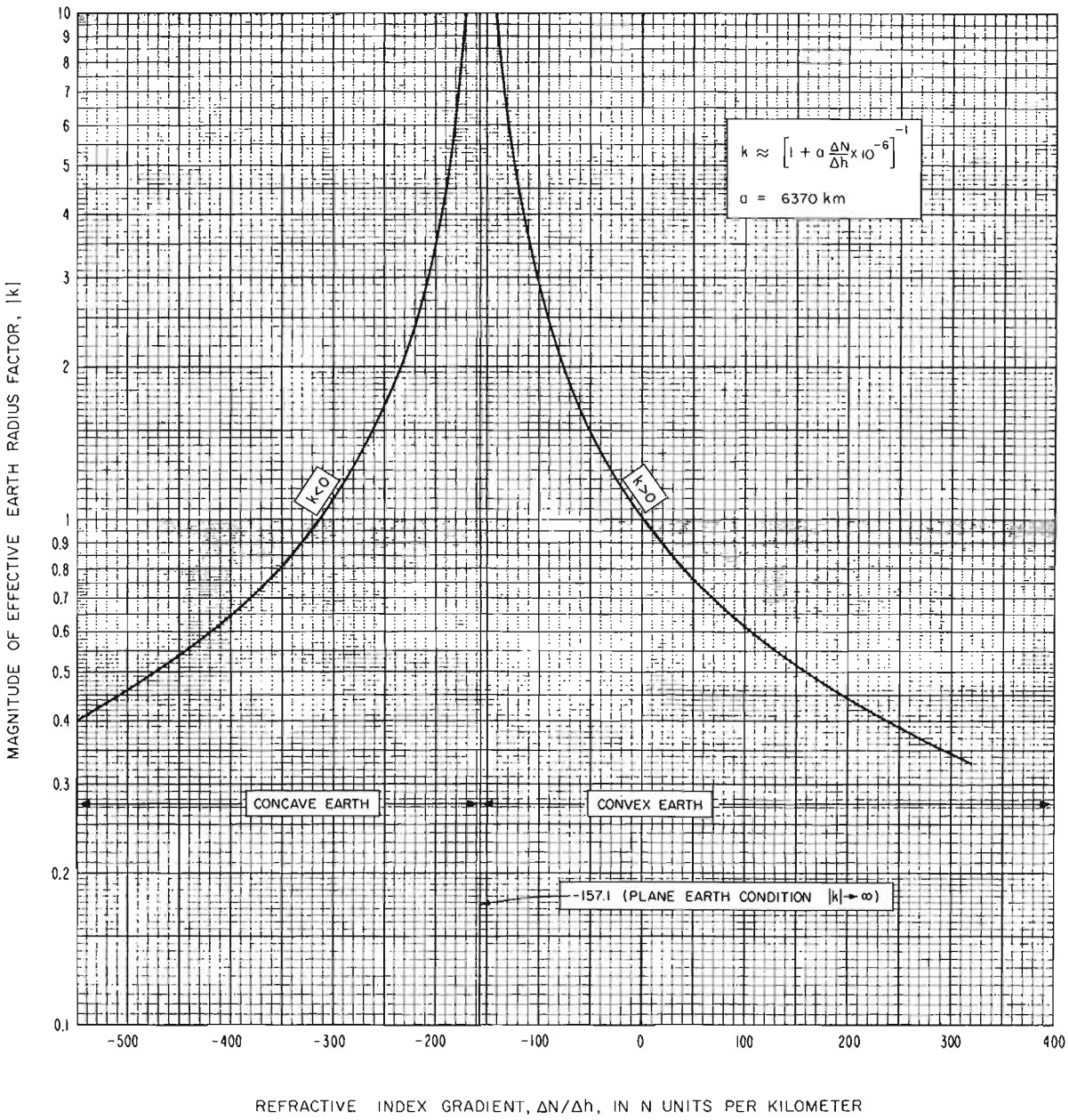

Figure 2

A DISTRIBUTION OF REFRACTIVE INDEX GRADIENTS AVERAGED OVER THE FIRST 50 AND 100 METERS ABOVE THE SURFACE

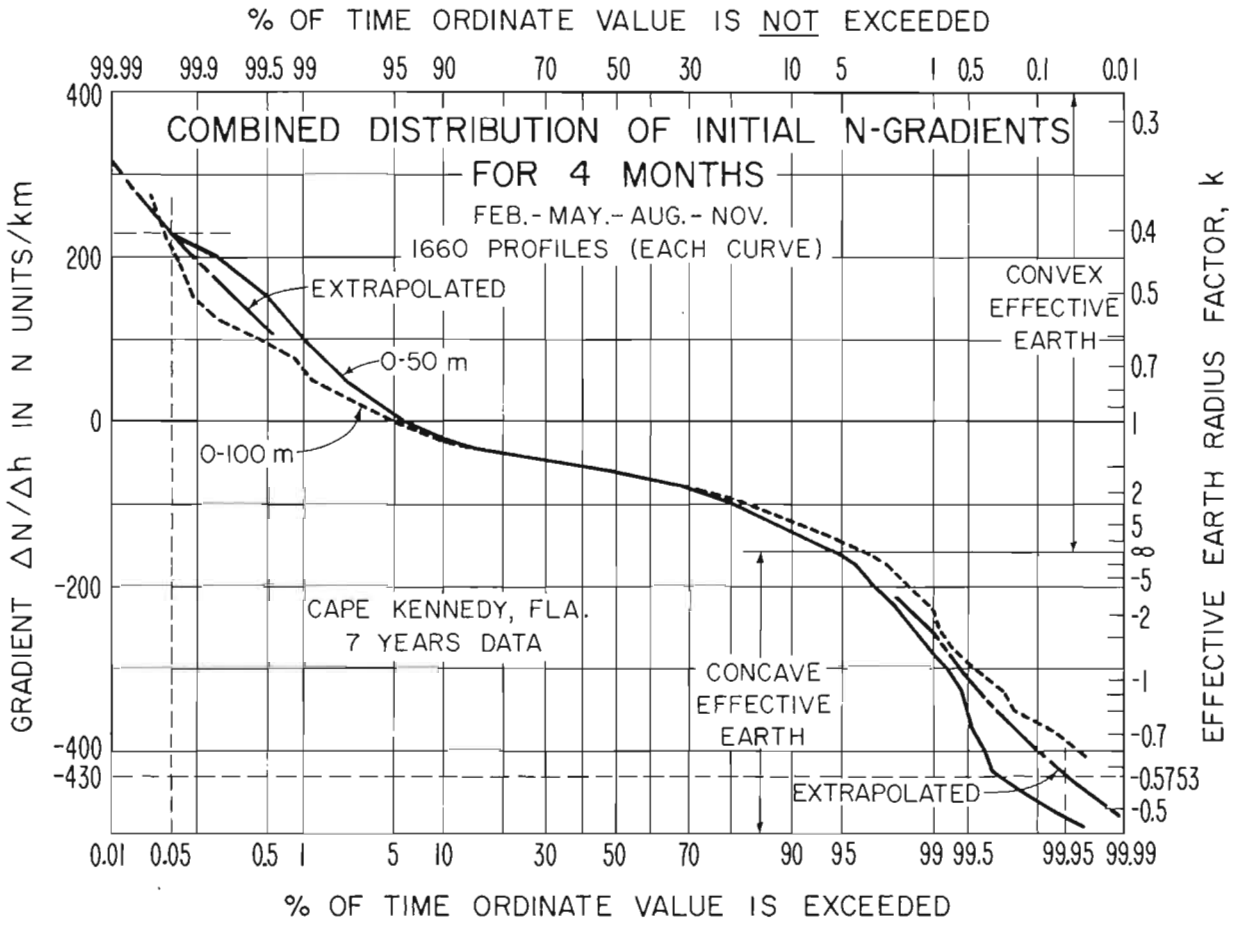

Figure 3

available information is included in a recent world atlas of refractive index gradients (Bean et al., 1966).

Note that the median value of figure 3 is approximately -60 N units/km, a departure from the commonly used median value of approximately -40 N units/km that is associated with the 4/3 earth. Such differences are generally negligible for transmission frequencies of several hundreds of megahertz, or less. At microwave frequencies, however, this difference can be significant. A similar situation exists in the plotting of propagation path profiles; a 4/3 earth path profile can be misleading--it corresponds to a situation that is not particularly significant for fading situations and can obscure the dynamic nature of microwave propagation through the lower atmosphere. Preferable procedures are available. For example, charts are commercially available for plotting the various ray paths between two terminals (such as in fig. 1) for a range of k values. This is applicable to any profile but avoids much computation when the profile is a simple rectangular height-versus-distance profile taken directly from a map.

The meteorological conditions that support the microwave fading mechanisms commonly take the form of marked departures from median conditions. Strong refractive index gradients occur over a limited range of elevation (layers) at, or above, the terrain surface. In most cases they can be associated with known meteorological processes and described in terms of typical geographical locations and weather conditions recognizable to the systems engineer. They also exhibit typical behavior in terms of meteorological measurements available from stations of the U.S. Weather Bureau and can be systematized for quick reference.

This is illustrated in figure 4, a schematic description of those superrefractive surface gradients that are caused by the radiation of heat from the surface to a clear sky. At night, clear skies and light surface winds permit considerable cooling of the earth's surface. This can cause the formation of a temperature inversion (an increase of temperature with height) and produce a strong superrefractive gradient near the surface--a condition that can dramatically affect microwave propagation.

The likelihood of extreme subrefractive or superrefractive gradients is reduced for propagation above rough terrain. Line-of-sight propagation paths between high points of mountainous terrain will, in general, experience more linear distributions of gradients with reduced standard deviations (compared to that depicted in fig. 3). They, therefore, exhibit only slight variations in signal level (Klein and Libois, 1953). There are exceptions to this, such as in the coastal range of mountains of northern Chile, which are attributable to the intrusion of the trade wind inversion among the mountain peaks. Similarly, the distribution of refractive index gradients exhibit a more negative median for oversea paths (Ikegami, 1964). A detailed, informative treatment of the refraction of radio waves and the refractive index structure of the lower atmosphere may be found in a recent U. S. Department of Commerce publication (Bean and Dutton, 1966).

3. FADING MECHANISMS

The significance of the refractive index structure for microwave fading is best illustrated by the variety of the propagation situations that produce such fading. Here we classify and illustrate these propagation fading mechanisms and identify the supporting refractive index structures. Only a general discussion of the fading signal characteristics and their remedies is provided; detailed treatments are deferred to subsequent sections.

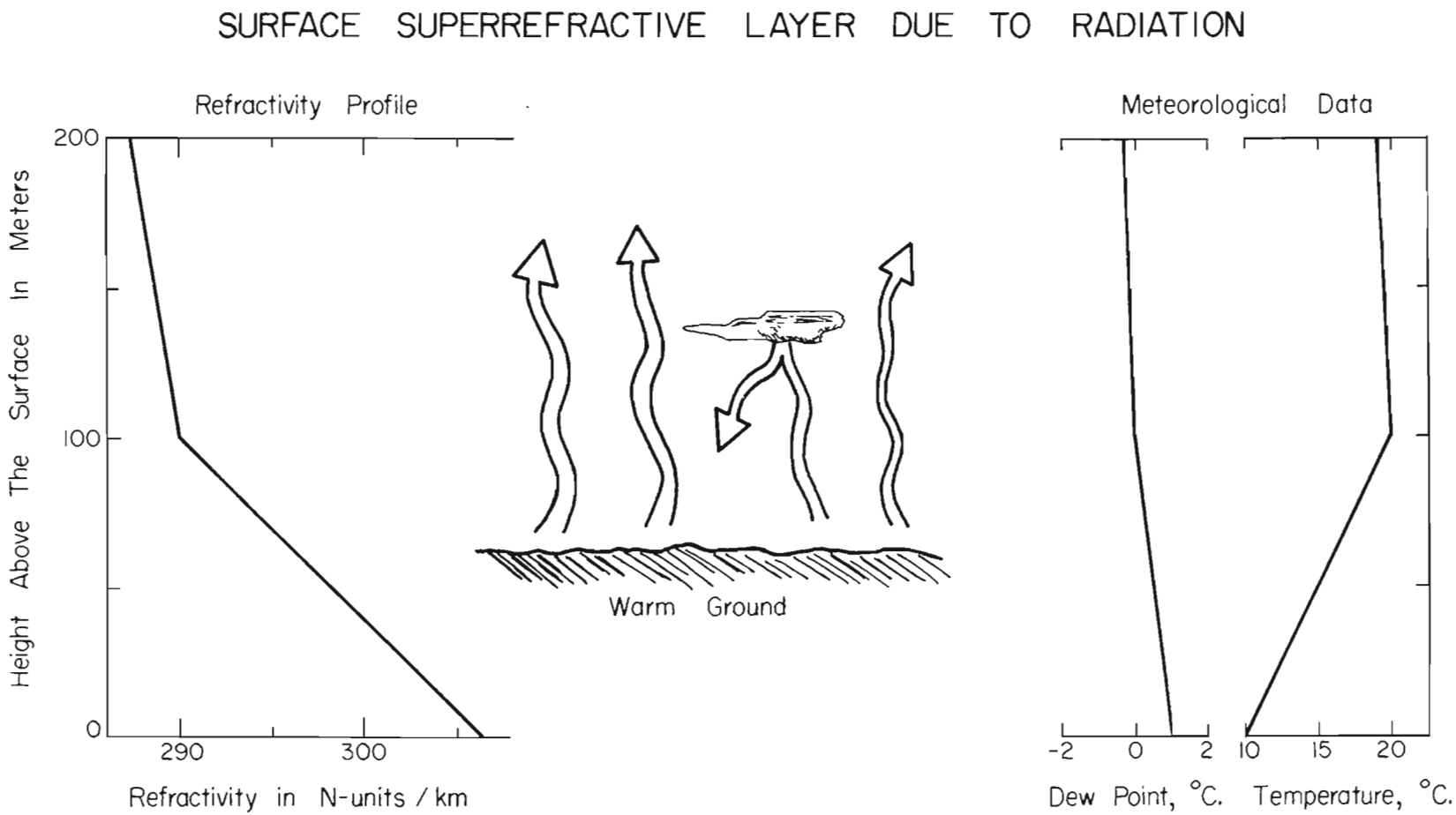

Figure 4.

OCCURRENCE: Clear skies and light surface winds at night permit a considerable cooling of the earth's surface due to the radiation of heat to space. The air near the surface also cools, resulting in a temperature inversion.

The fading experienced at microwave frequencies for tropospheric line-of-sight paths may be considered under two general categories: multipath fading and power fading. Each category includes several fading mechanisms that exhibit characteristics that often permit their identification.

3.1. Multipath Fading

As the refractive index gradient varies, multipath fading results from interference between the direct wave and

(a) the specular component of the ground-reflected wave;

(b) the nonspecular component of the ground-reflected wave;

(c) partial reflections from atmospheric sheets or elevated layers; or

(d) additional direct (nonreflected) wave paths.

These additional direct wave paths can occur due to either the surface layers of strong positive refractive index gradients (Magnuski, 1956; Nicolis, 1966) or the horizontally distributed changes in refractive index--as may be encountered with a weather front (Misme, 1957). The multipath fading mechanisms are illustrated in figure 5.

The depths of fades encountered for these multipath phenomena can be quite severe, depending upon the effective reflection coefficients or the relative amplitudes of the component waves. Mechanisms (a) and (c) can produce fades persisting for minutes. During such fades the nonspecular ground-reflected components (normally small for small grazing angles) can cause additional interference (with the direct plus specular component), providing even deeper, more rapid, fades having durations of the order of seconds. An illustration of multipath fading (direct plus ground-reflected wave) is presented in figure 6 to show the characteristic return of signal level to, or above, the free-space value. In figure 6, a basic transmission loss (Rice et al., 1966)

MULTIPATH FADING MECHANISMS

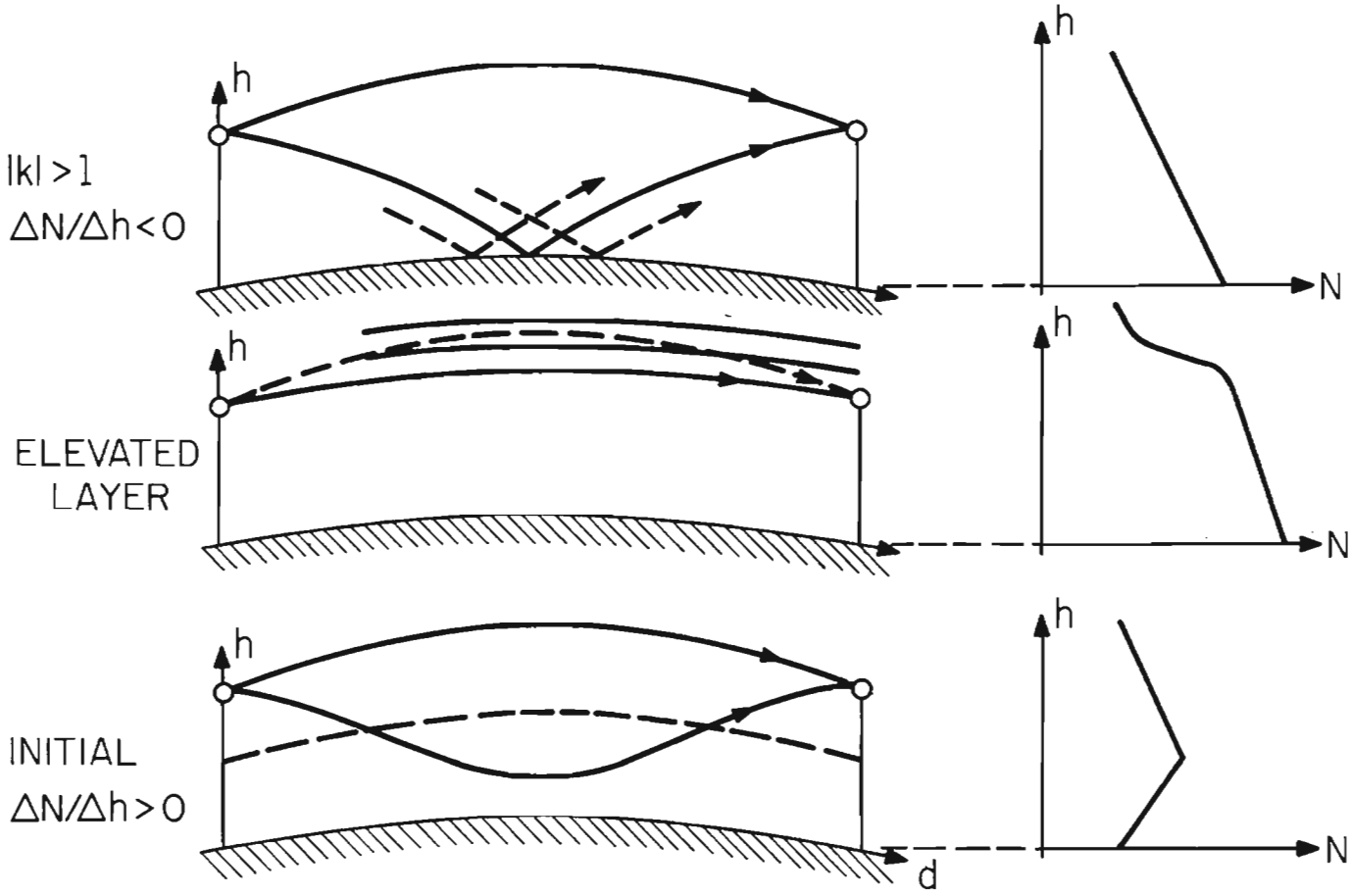

Figure 5

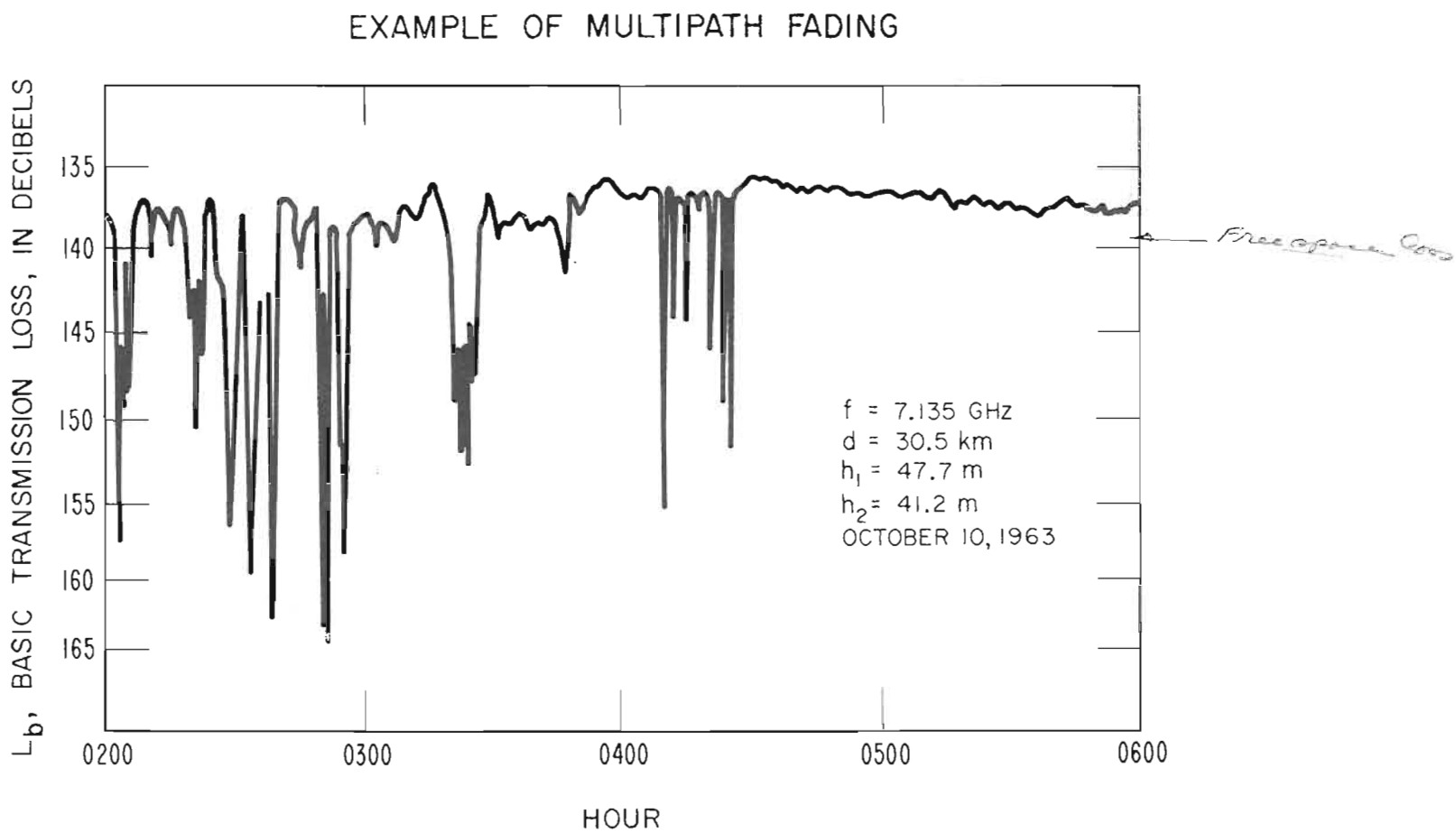
EXAMPLE OF MULTIPATH FADING
L_b, BASIC TRANSMISSION LOSS, IN DECIBELS
135
140
145
150
155
160
165
0200
0300
0400
0500
0600
HOUR
f = 7.135 GHz
d = 30.5 km
h_1 = 47.7 m
h_2 = 41.2 m
OCTOBER 10, 1963
Free space loss

Figure 6

of approximately 139 dB corresponds to that for the free-space signal level. The multipath fading tends to be less frequent during the day, particularly during the afternoon hours, when conditions more closely approach a median or reference atmospheric structure, a condition for which most paths are designed.

Figure 7 presents an illustration of the frequency selectivity of multipath fading. There, the recordings of received signals of two transmission frequencies are presented for a common propagation path. On an instantaneous basis the two recordings appear uncorrelated. Note, however, that with an allowance for time lag the two signals are highly correlated. This time lag for high correlation, which is a measure of the effective (frequency) diversity separation, is a function not only of the frequency separation, but also of the refractive index gradient and its time rate of change. Clearly, the frequency spacing of figure 7 is inadequate if fades of 20 dB below the 139-dB free-space level are unacceptable.

The multipath fading due to the interference from specular ground reflections can be avoided by eliminating one of the field components. The specularly reflected wave can be severely reduced by special "anti-reflective wave" antenna arrays (Bateman, 1946; Kawazu et al., 1959) or by the use of Fresnel zone screens (Bussey, 1950; Ugai, et al., 1963; Preikschat, 1964). These devices assume that the range of refractive index gradients will not be too wide. For propagation over rough irregular terrain, this last condition is usually met, and the effects of ground reflections may then be avoided by the proper choice of antenna sites or antenna designs. To date, however, the most effective counter measure for general multipath fading over wide ranges of refractive index gradients is diversity reception (Cabessa, 1955; Magnuski, 1956; Lewin, 1962; Albertson, 1964). This will be treated in further detail in section 5.

EXAMPLE OF FREQUENCY SELECTIVITY
FOR MULTIPATH FADING

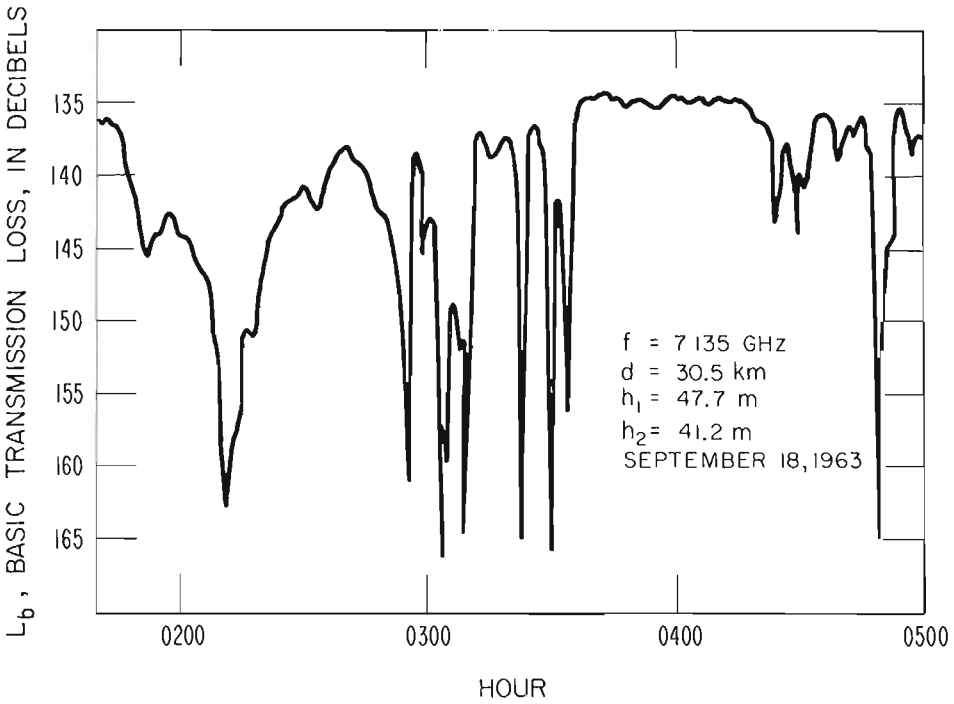

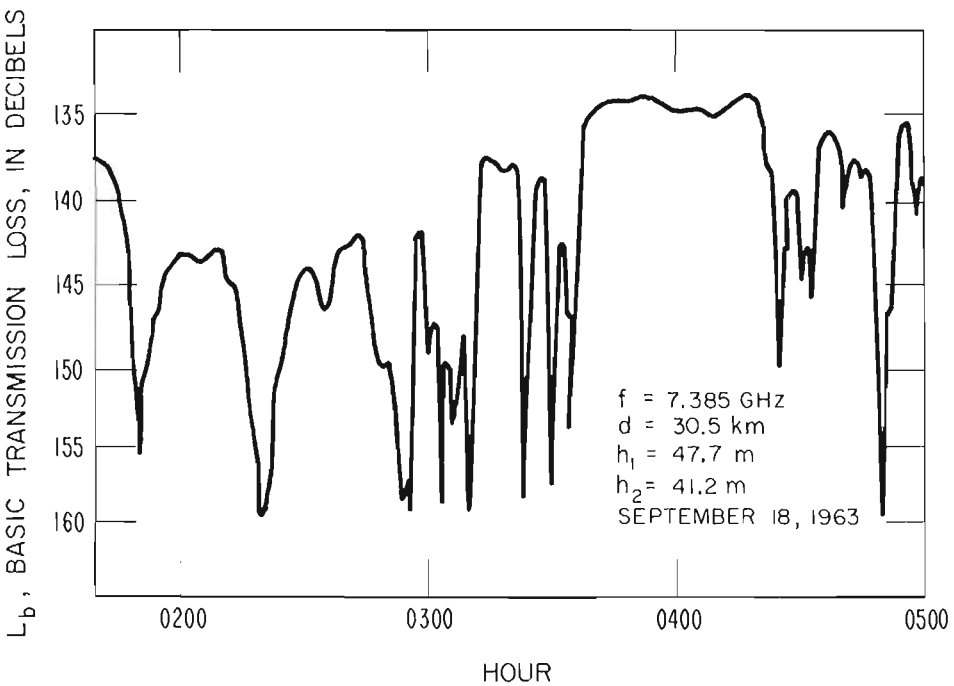

Figure 7

3.2. Power Fading

Power fading results from the partial isolation of the transmitting and receiving antennas because of:

(a) intrusion of the earth's surface or atmospheric layers into the propagation path (earth-bulge fading or diffraction fading*);

(b) antenna decoupling due to variation of the refractive index gradient;

(c) partial reflection from elevated layers interpositioned between the terminal antenna elevations;

(d) "ducting" formations containing only one of the terminal antennas; and

(e) precipitation along the propagation path (Ryde and Ryde, 1945; Hunter, 1964; Medhurst, 1965; Kuhn, 1967).

The received signal for these power fading mechanisms is characterized by a marked decrease in median signal level below that for free space and for extended periods of time. Some examples of these fading mechanisms are given in figure 8.

* When a strong atmospheric layer intrudes into the direct propagation path between transmitter and receiver, the effect is much like that for intrusion of the earth's surface. For example, the energy represented by ray paths which strike the surface of a superrefractive layer, at grazing angles of more than a few milliradians, penetrates the layer and is diverted from the direct path to the receiver location. The ray path at grazing incidence and those ray paths which pass above the layer provide a contribution to the receiver in the radio hole or "shadow" of the layer via the diffracted mode of propagation. The received field may be determined by applying the Leontovitch boundary conditions at grazing incidence where $n^2 - 1 << 1$ (Hufford, 1952).

ATTENUATION FADING MECHANISMS

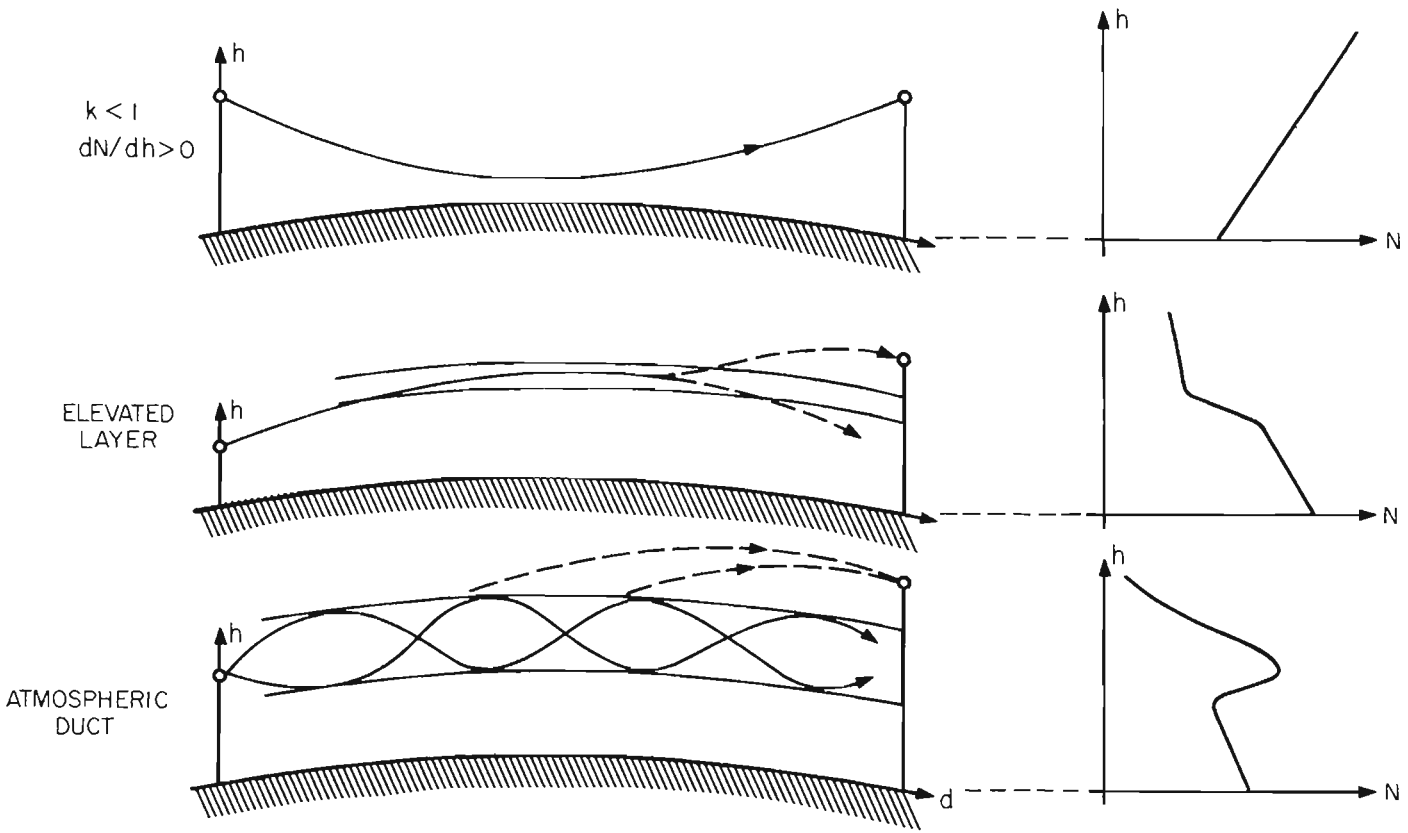

Figure 8

3.2.1. Power Fading Due to Diffraction

The power fades that occur due to diffraction by the earth's surface are generally supported by a subrefractive (positive) gradient of refractive index. The situation is illustrated by the upper diagram of figure 8. This type of fading can persist for several hours and to depths of 20 or 30 dB. The fading is essentially independent of small scale changes of frequency, but may be reduced or avoided by a proper choice of terminal antenna heights.

In mountainous terrain where terminals are located on dominating ridges or peaks, a single Fresnel zone clearance, or even less, will usually be sufficient. The clearance corresponding to n Fresnel zones in meters is

$$C_n = 8.66 \sqrt{nd/f}, \tag{4}$$

where the path length d is in kilometers and the transmission frequency f is gigahertz. If only a limited range of refractive index gradients is encountered, a first Fresnel zone clearance, C_1, or less is sufficient (Klein and Libois, 1953; Troitskii, 1960). For those microwave paths where subrefractive index gradients are encountered, increased clearances are required. Consider a 2-GHz, 50-km propagation path with terminal antennas at equal heights. The smooth spherical earth diffraction loss for such a path is shown in figure 9 as a function of antenna height and path length when the refractive index gradient is 80 N units/km. The path length d in kilometers, the effective earth radius factor k (related to the gradient $\Delta N/\Delta h$ through (3)), and the antenna heights, h_1 and h_2 in meters, for which the path would be just grazing (i.e., barely line of sight) are related by

$$d = \sqrt{12.74\, kh_1} + \sqrt{12.74\, kh_2} \tag{5}$$

ATTENUATION CURVES FOR A 2-GHz PROPAGATION PATH

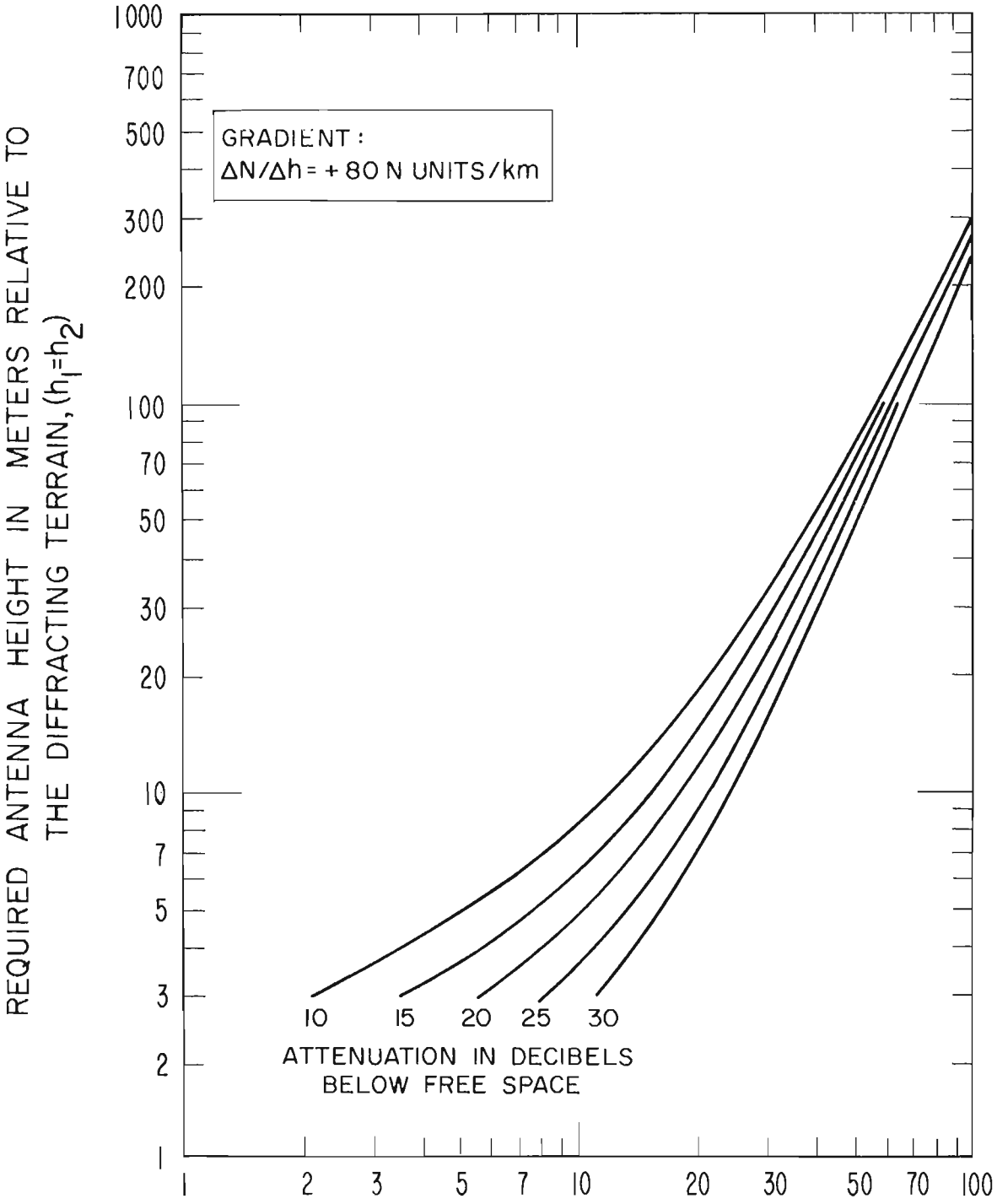

Figure 9.

This expression involves the familiar relation between antenna height and horizon distance over smooth earth, modified here for the metric system of units. The path would be just barely line-of-sight for k = 4/3 in (5) when the antenna heights were $h_1 = h_2 = 36.73$ m. A first Fresnel zone clearance, $C_1 = 43.3$ m from (4), would therefore require terminal antenna heights of 80 m. Such a path would, however, still experience an attenuation of 10 dB for $\Delta N/\Delta h = 80$ N units/km (see fig. 9) and 23 dB for $\Delta N/\Delta h = 160$ N units/km. To protect against a particular depth of diffraction fading, we must specify the clearance in terms of the subrefractive gradients that may be encountered and the shape of the obstructing terrain. Dougherty and Wilkerson (1967) have recently presented a design procedure for determining the antenna heights required for adequate protection.

Diffraction fading in the sense used earlier may also occur when a strong superrefractive layer is positioned slightly below the terminal antennas (Dutton, 1961). This was described in the footnote on p. 17 and is illustrated in figure 10. In such a situation the grazing condition is given by (5) when the h_1 and h_2 are the heights of the antennas above the top of the layer and k corresponds to the average gradient between each antenna and the top of the layer. This situation is known as a radio hole in air-to-air applications (Doherty, 1952; Dougherty, 1967). The fading loss can be severe and may be estimated at grazing from figure 11 (Dougherty and Wilkerson, 1967). The severity of this type of fading will be reduced somewhat by terrain reflections or contributions from subrefractive layers positioned below the diffracting layer, which can direct energy back toward the receiver. These contributions, indicated in figure 10, are a function of the gradients within and below the diffracting layer and also of the terrain roughness.

DIFFRACTION FADING DUE TO LAYERING

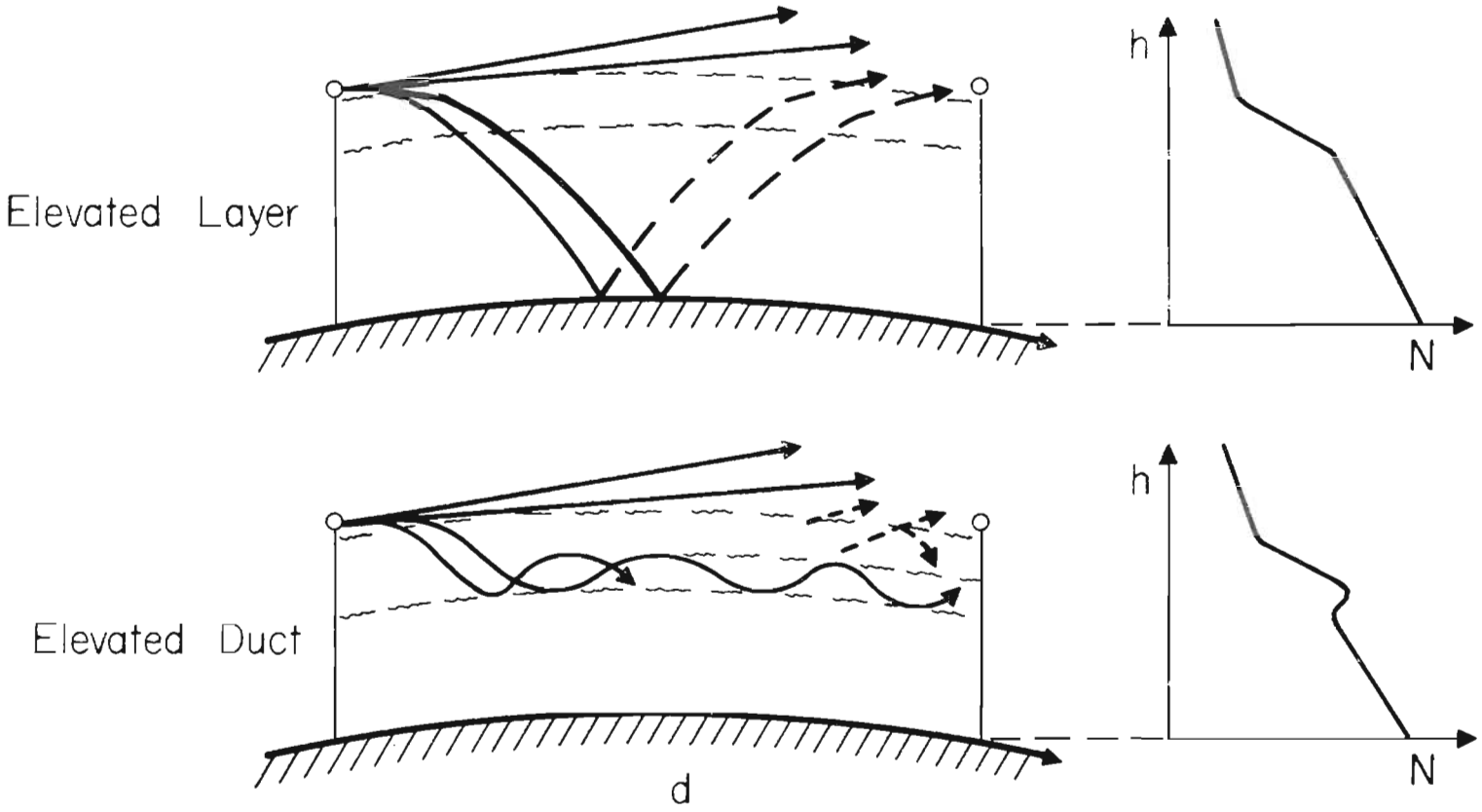

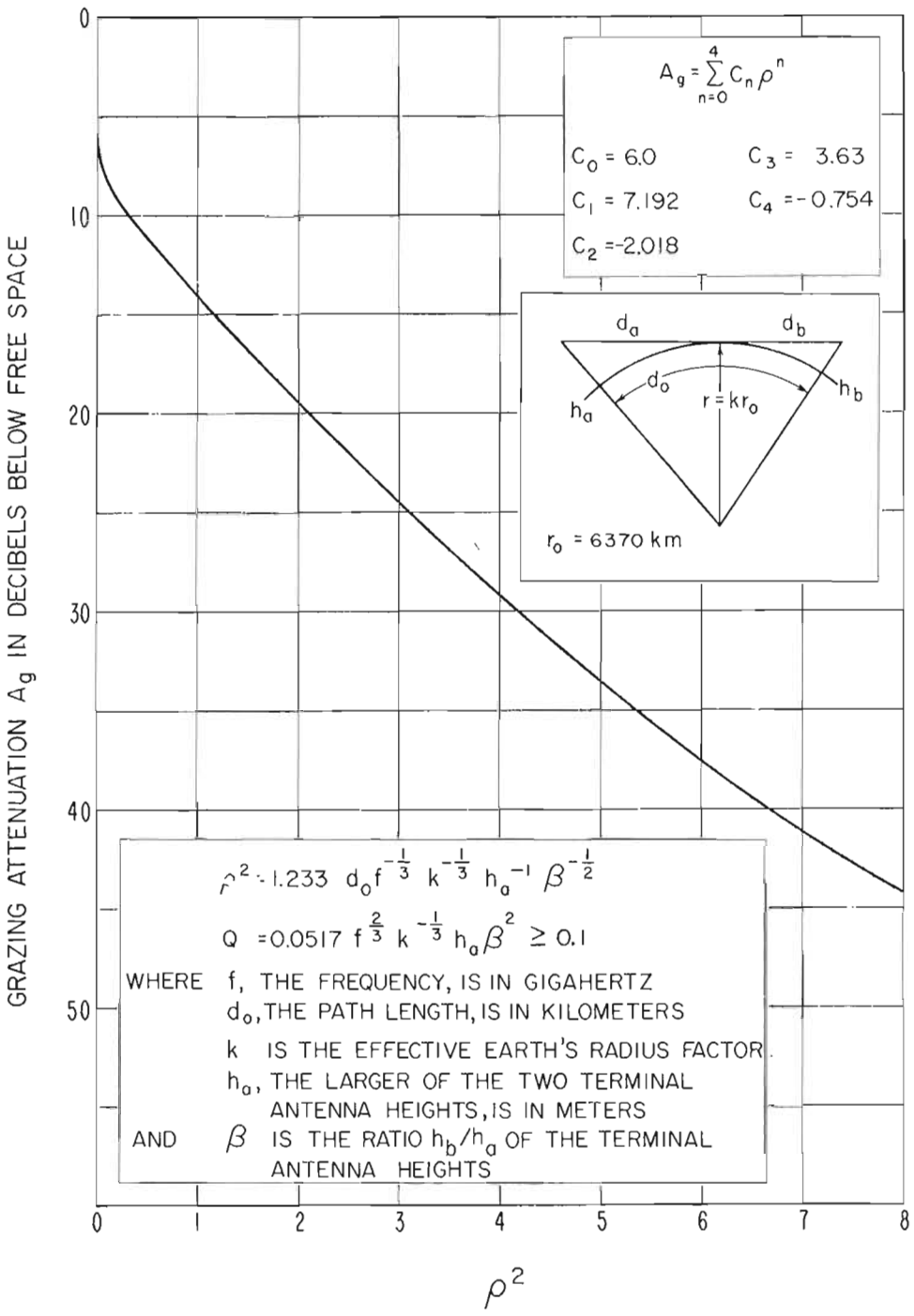
ATTENUATION OF A FIELD DUE TO
DIFFRACTION BY A SMOOTH SPHERICAL EARTH
AT EXACTLY GRAZING CONDITIONS AND
RELATIVE TO THE FREE SPACE FIELD
GRAZING ATTENUATION A_g IN DECIBELS BELOW FREE SPACE
$A_g = \sum_{n=0}^{4} C_n \rho^n$
C_0 = 6.0
C_1 = 7.192
C_2 = -2.018
C_3 = 3.63
C_4 = -0.754
d_a
d_b
d_o
h_a
h_b
$r = kr_o$
r_o = 6370 km
$\rho^2 = 1.233\ d_o f^{-\frac{1}{3}} k^{-\frac{1}{3}} h_a^{-1} \beta^{-\frac{1}{2}}$
$Q = 0.0517\ f^{\frac{2}{3}} k^{-\frac{1}{3}} h_a \beta^2 \geq 0.1$
WHERE f, THE FREQUENCY, IS IN GIGAHERTZ
d_o, THE PATH LENGTH, IS IN KILOMETERS
k IS THE EFFECTIVE EARTH'S RADIUS FACTOR.
h_a, THE LARGER OF THE TWO TERMINAL ANTENNA HEIGHTS, IS IN METERS
AND β IS THE RATIO h_b/h_a OF THE TERMINAL ANTENNA HEIGHTS
0
10
20
30
40
50
0
1
2
3
4
5
6
7
8
ρ^2

Figure 11

3.2.2. Power Fading Due to Antenna "Decoupling"

Power fading due to antenna "decoupling" refers to the loss of signal that occurs for transmission and reception of the signal outside of, or at the extremeties of, the main lobe of the antenna pattern. For example, Sharpless (1946) observed variations in the vertical angle of arrival of up to 0.5° on a 38.6-km line-of-sight path. This effect is proportional to the path length and can introduce several decibels of loss for high gain antennas and long line-of-sight paths. This loss may be minimized by specifying a sufficiently broad antenna beam so that the expected variations of the angle of arrival are matched or exceeded. This variation is most conveniently expressed relative to the angle-of-arrival for flat earth, $k = \infty$, conditions. Thus, at the terminal whose antenna elevation is H_1 m, the angle of arrival from an antenna at an elevation of H_2 m and d_0 km distant, is given (for $k = \infty$) by

$$\tan \theta_1(k = \infty) = \left[(H_2 - H_1)/ d_0\right] 10^{-3} , \qquad (6a)$$

or, for most practical situations where θ_1, is small,

$$\theta_1(\infty) \approx (H_2 - H_1)/d_0 \text{ mrad.} \qquad (6b)$$

For situations that may be approximated by a linear gradient, k is given by (3) and the angle of arrival will be

$$\tan \theta_1(k) = -79 \times 10^{-6} [d_0/k] + \tan \theta_1(\infty) , \qquad (6c)$$

or

$$\theta_1(k) - \theta_1(\infty) \approx -0.079\, d_0/k \text{ mrad} \qquad (6d)$$

$$\approx -0.0045\, d_0/k^{\circ} , \qquad (6e)$$

as derived in the appendix.

For high gain antennas, superrefractive conditions (negative k values) will tend to enhance the reception of ground reflected rays, and subrefractive conditions (positive k values less than unity) will tend to enhance the contributions from elevated layers, etc. This should be clear from (6c), since k is positive and greater than unity for common design practice. Negative k-values then cause the angle of arrival to exceed that for which the antennas are oriented. Similarly, for $0 < k < 1.0$, the angle of arrival is less than that for the design conditions.

3.2.3. Power Fading Due to Ducts and Layers

The power fading due to atmospheric ducts and elevated layers, (c) and (d) in 3.2., are characterized by fades of 20 dB and occasionally over greater values. They may persist for hours or days, but tend to be less frequent during daylight hours. This type of fading mechanism is the likely source of many space-wave fadeouts (Bean, 1954; Barsis and Johnson, 1961; 1962). The fading is not generally sensitive to small-scale (in-band) changes of frequency or of spatial position of the antennas, and cannot therefore readily be remedied by commonly used diversity techniques.

The elevated duct is sometimes a combination of elevated layers, and is described by the occurrence of a superrefractive layer above a subrefractive layer. This has the effect of guiding or focusing the signal energy along the duct. The reverse can also occur; the combination of a subrefractive layer above a superrefractive layer will defocus energy introduced within the combination of layers. For terminals within such a combination, the defocusing effect will produce a power fade (Wilkerson, 1962; Nicolis, 1967).

Obviously, repositioning of one or both antennas can eliminate the problem--see the two lower diagrams of figure 8--and in some situations this is feasible (Dawson, 1961), although major height changes may be required. For effective repositioning of the antennas, some information about layer characteristics (prevalence, thickness, height, etc.) is required (Dutton, 1961; Cahoon and Riggs, 1964; Bean et al., 1966). For example, the likelihood of isolation is reduced, for long paths, by locating both terminal antennas at the same height relative to the expected duct or layer position. For short paths, however, the likelihood of isolation is reduced by a difference in antenna heights which must be sufficient to insure that the angle of incidence at the elevated layer is on the order of a few degrees.

3.2.4. Fading Due to Precipitation

Power fading can also occur due to signal attenuation by extensive precipitation along a propagation path (Ryde and Ryde, 1945). The effects of this fading are avoided by route diversity, the use of an alternate series of communication links (Murray and Flager, 1965; Hogg, 1967).

3.3. Combinations of Fading Mechanisms

For many propagation paths, more than one fading mechanism will be involved, their relative significance changing with the refractive index. Two particular combinations that can be especially troublesome are k-type fading as described below, and surface-duct fading.

3.3.1. K-Type Fading

The k-type fading occurs for propagation over smooth or uniformly irregular terrain such as the sea surface, maritime terrain or gently rolling (pastoral) terrain. The mechanism involves either the

multipath fading (direct ray plus ground reflections) or the diffraction type of power fading depending upon the value k of the earth-radius factor (Matsuo et al., 1953). The two mechanisms supplement one another, insuring a source of fading throughout a wide range of refractive index gradients or k values. Resulting signal variations are illustrated in figure 12, the spherical-earth transmission loss versus refractive index gradient, which also shows the effect of terrain roughness (expressed by σ/λ) and the divergence-convergence factor under the dynamic influence of the refractive index gradient. The ratio σ/λ is that of the standard deviation of the surface irregularities, σ, (about a median spherical surface) to the transmission wavelength, λ. For a smooth earth ($\sigma/\lambda = 0$), the fading, marked by the nulls of interference between the direct wave and the specularly reflected wave, is serious only over a limited range of refractive index gradients. For the path parameters of figure 12, as an example, the fades due to the interference nulls can exceed 20 dB only within the range of -115 to -195 N units/km and for gradients in excess of 300 N units/km. As the surface roughness is increased, $\sigma/\lambda > 0$ (Beckmann and Spizzichino, 1963) and the critical region of gradients shifts to more negative values. In figure 12, for example, the critical region for negative gradients shifts to the range -180 to -290 N units/km, for $\sigma/\lambda = 10$. Irregularities or roughness that would cause the median terrain surface to depart slightly from a sphere could also shift the range of critical negative gradients in either direction. These critical ranges, as well as those due to the diffraction fade (at values greater than 300 N units/km), depend upon the specific link parameters (transmission frequency, antenna height, and path length). One aspect should be clear from figure 12: unless the terrain roughness is sufficient to shift the critical

ILLUSTRATION OF THE VARIATION OF FIELD STRENGTH WITH REFRACTIVE INDEX GRADIENT, k-TYPE FADING

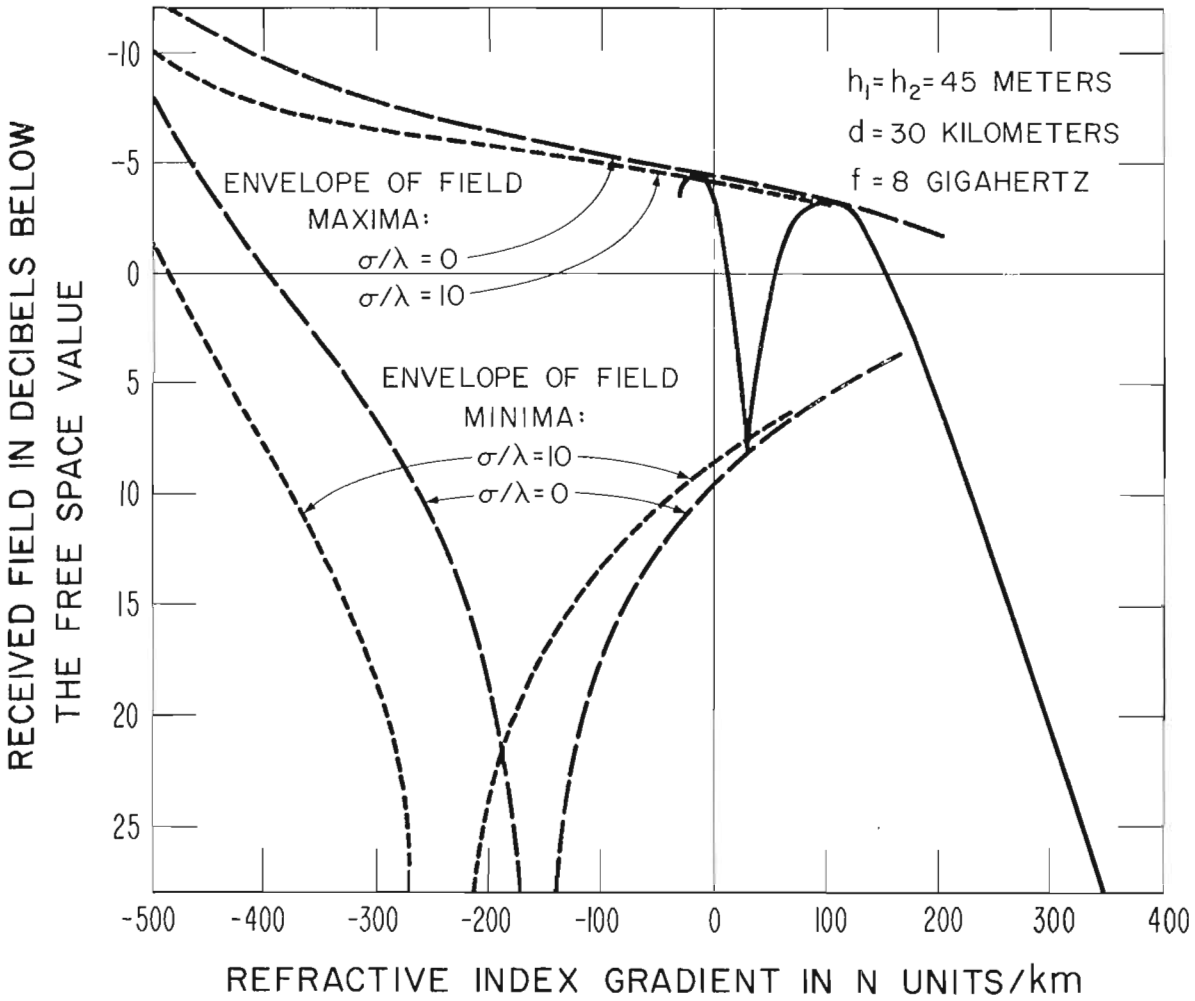

Figure 12

range of negative gradients outside of the range of refractive index gradients expected to occur at a particular location (see fig. 3, for example), reflections from the terrain surface cannot be neglected. Similarly, high points of the terrain cannot be considered to eliminate terrain reflection unless they also partially obstruct the reflected wave over the critical range of refractive index gradients.

The effects of k-type fading are reduced by (a) increasing the terminal antenna heights to provide adequate protection against the diffraction fading for the expected extreme positive gradients of refractive index; and also (b) diversity reception that effectively reduces the attenuation due to multipath out to the expected extreme negative gradients of refractive index. Such a design procedure was first proposed and demonstrated by Lewin (1962). Dougherty and Wilkerson (1967) and Norton et al. (in an unpublished 1965 report) have provided a more accurate extension to Lewin's design.

3.3.2. Surface Duct Fading

Surface duct fading is encountered on long, line-of-sight, over-water paths and is due to the presence of surface ducts. These sea surface ducts may constitute a semipermanent condition as, for example, in the region of the Bermuda High, a high-pressure region of the Atlantic between 10 and 30° N latitude. There, the ducts form less than 2 km from the shore and extend from the sea surface up to heights of 7 to 20 m, for wind velocities from 15 to 55 km/hr, persisting during fair weather and reforming after squalls and rain showers (Katzin et al., 1947). The fading mechanism is a combination of multipath fading (for reflections from the sea) and power fading in the presence of the sea surface duct. Two situations are illustrated in figure 13. Because of the continual disturbance of the sea surface, a reflected wave

SURFACE DUCT FADING MECHANISM

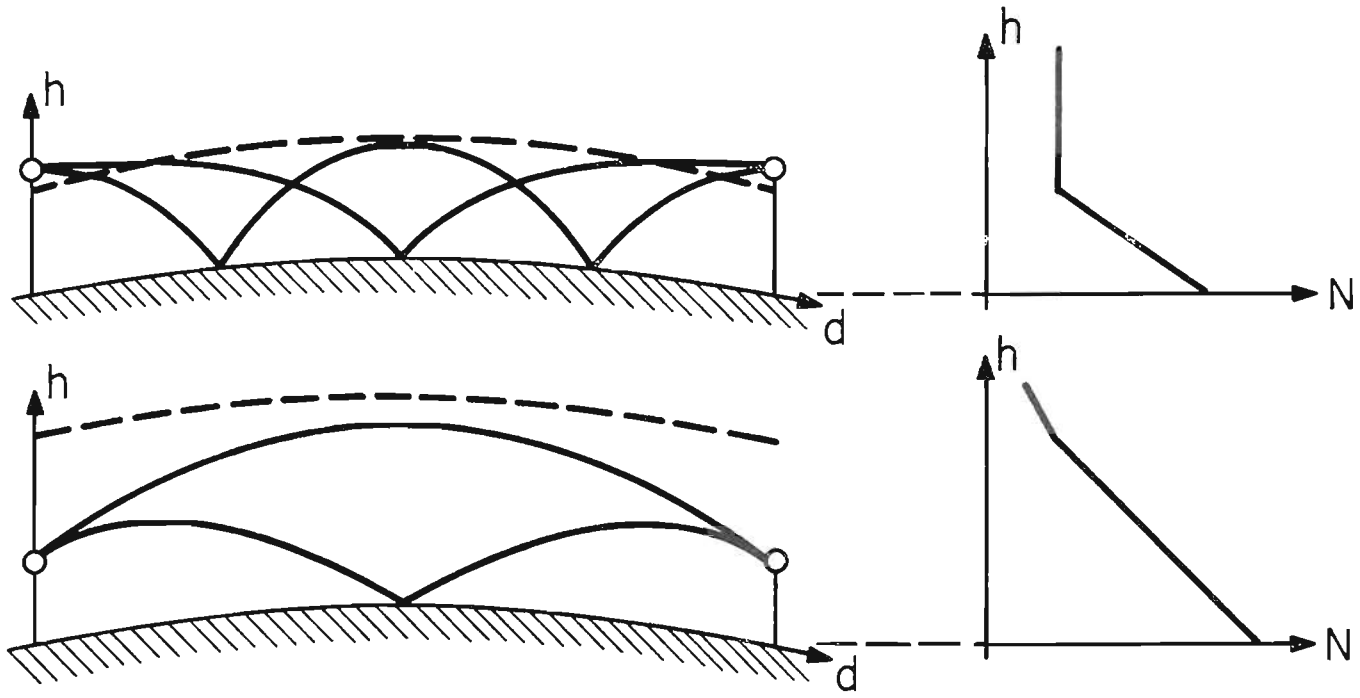

Figure 13

consists of a diffuse or randomly distributed component superimposed upon the specular component. This time distribution of the reflected wave is a Beckmann distribution--a constant plus a Hoyt distribution (Hoyt, 1947; Beckmann, 1962, 1963). This constitutes the received field for the upper diagram of figure 13. Addition of the direct wave, as in the situation illustrated by the lower diagram of figure 13, produces an enhanced or reduced constant component due to phase interference. One effect of the surface duct upon the multipath situation is to provide an increased angle of incidence. This increases the ratio of the diffused to specular amplitudes, and increases the rapidly varying component of the reflected signal. The net result is a total signal whose distribution approaches the Nakagami-Rice distribution, a constant plus a Rayleigh-distributed variable (Nakagami, 1943, 1964; Rice, 1944, 1945; Norton et al., 1955; Burns, 1964).

These surface or ground-based ducts guide or trap the radio waves by the combination of a strong negative refractive index gradient (superrefraction, $\Delta N/\Delta h \leq -157$ N units/km) and a reflecting sea or ground. As such, propagation within the duct has been described by Furutsu (1965) in terms of an equivalent linear gradient of refractive index. The corresponding equivalent earth representation is shown in figure 14. The field results from phase interference between a direct wave, one to three singly reflected waves, and, for sufficiently strong superrefraction, doubly reflected waves.

Surface-duct fading can also be reduced by means of a proper adaptation of Lewin's procedure. Choosing the initial terminal antenna heights to provide adequate Fresnel zone clearance (above the ducting layer) avoids the situation shown in the upper drawing in figure 13. Similarly, lower antenna heights could achieve the situation shown in the lower drawing of figure 13. In the latter case, diversity reception would also be required.

EXAMPLES OF SURFACE DUCT PROPAGATION FOR EFFECTIVE EARTH RADIUS AND TRUE EARTH RADIUS

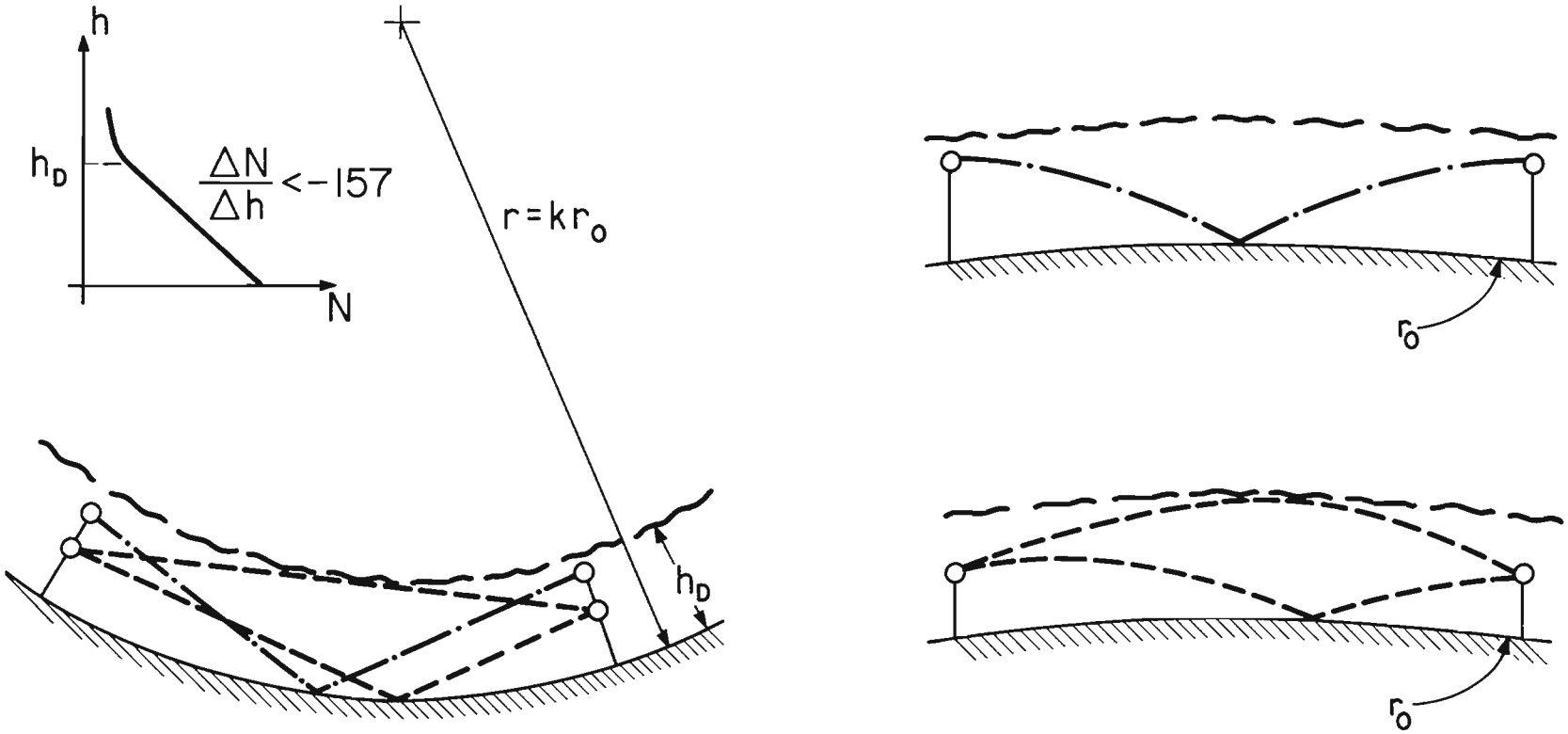

Figure 14

4. DISTRIBUTION CURVES FOR MULTIPATH FADING

The commonly accepted sources of multipath fading are those due to reflection from the (sea or land) surfaces or from layering in the atmosphere. Such multipath produces amplitude distributions of the received signal that are characterized by several features. First, the maximum signal between fades exceeds, to some extent, the free space level. Second, the signal exhibits a frequency and duration of fades which are related not only to the path geometry and transmission frequency, but also to the variation of the refractive index structure with time. Third, the multipath signal distribution is one of a specific family of distributions. This section provides, where possible, a quantitative description of these characteristics and thereby a means of identifying the probable causes of fading when fading is observed.

4.1. The Relative Amplitudes of the Multipath Components

The peak values of multipath signal distributions depend upon the number of signal components and their relative amplitudes--specifically, the algebraic sum of all components. Similarly, the number and relative amplitude of the components and their phases determine the distribution of their vector sum. The first requirement, therefore, is a description of the relative amplitudes and phases of the components. This is not practical, at present, for all of the situations of interest. For example, there have been significant advances in the theoretical treatment of reflection or scattering from atmospheric layers in terms of specific refractive index profiles (Brekhovskikh, 1960; DuCastel et al., 1960; and Wait, 1962). In addition, experimental investigations (Bean, Frank, and Lane, 1963; Wait, 1964; Bean and Warner, 1965) have been reported. The state-of-the-art has not provided engineering expressions for the

expected magnitude and phase of the multipath components which, at microwave frequencies, are attributable to subrefractive or superrefractive layers in the atmosphere. We can, however, identify the distributions of signal amplitudes that would be expected; they coincide with those encountered for multipath produced by reflection and scattering from irregular terrain as described below.

There is an even longer history of theoretical and experimental studies of reflection and scattering from terrain. This has just recently resulted in engineering expressions that permit an estimate of the reflected and scattered components due to terrain (Beckmann and Spizzichino, 1963). For the particular case of small angles of incidence and the microwave frequencies at which specular reflection from terrain results in significant fading, the Fresnel reflection coefficients modified by a divergence factor may be taken as essentially unity (with a 180° phase shift upon reflection). The specular reflection coefficient then becomes equal to the factor given by Beckmann and Spizzichino (1963)

$$\alpha = \exp\{-g/2\} . \tag{7a}$$

Here,

$$g = \left[4\pi \frac{\sigma}{\lambda} \sin\theta\right]^2 , \tag{7b}$$

where σ is the standard deviation of the irregular terrain about its mean elevation, λ is the transmission wave length, and θ is the angle of incidence (zero for grazing conditions). The expression for g is recognizable as related to the Rayleigh criterion for roughness. The specularly reflected component is therefore given by $\alpha\sqrt{G}$, where G is the geometric mean of the transmitting and receiving antenna power gain values for the reflected ray path. In addition to this specularly reflected component,

there is the random field scattered by the irregularities of the atmosphere and/or the reflecting terrain. The rms value of this nonspecularly reflected component depends upon the reflecting surface's distribution and correlation function, but is almost always appreciably less than

$$[G - a^2]^{\frac{1}{2}} \quad . \tag{7c}$$

4.2. The Received Signal Amplitude Distributions

In general, the multipath fading mechanisms produce two or more components with varying relative phases. Even when several components are involved, one or two of them tend to be dominant. For this reason,one would generally not expect a Rayleigh-distributed received signal. The departure from a Rayleigh distribution will take one of two forms, depending upon the nature of the field components.

For grazing angles of more than a few milliradians, the specularly reflected wave tends to be small,while the randomly (nonspecularly) reflected components tend to provide a significant contribution. The signal distribution tends to be less steep than a Rayleigh distribution; it consists of a constant direct signal plus a random signal (Nakagami, 1964; Beckmann, 1964). The resulting family of distributions, adapted from Beckmann (1962) and Beckmann and Spizzichino (1963), is illustrated in figures 15a through 15e as a function of the parameters B and K. These distributions give the percent of the time that the total signal r will exceed the rms value $\tilde{r}$ by an amount given by the vertical decibel scale. That is,

$$Z = 20 \log_{10}(r/\tilde{r}) \quad . \tag{8}$$

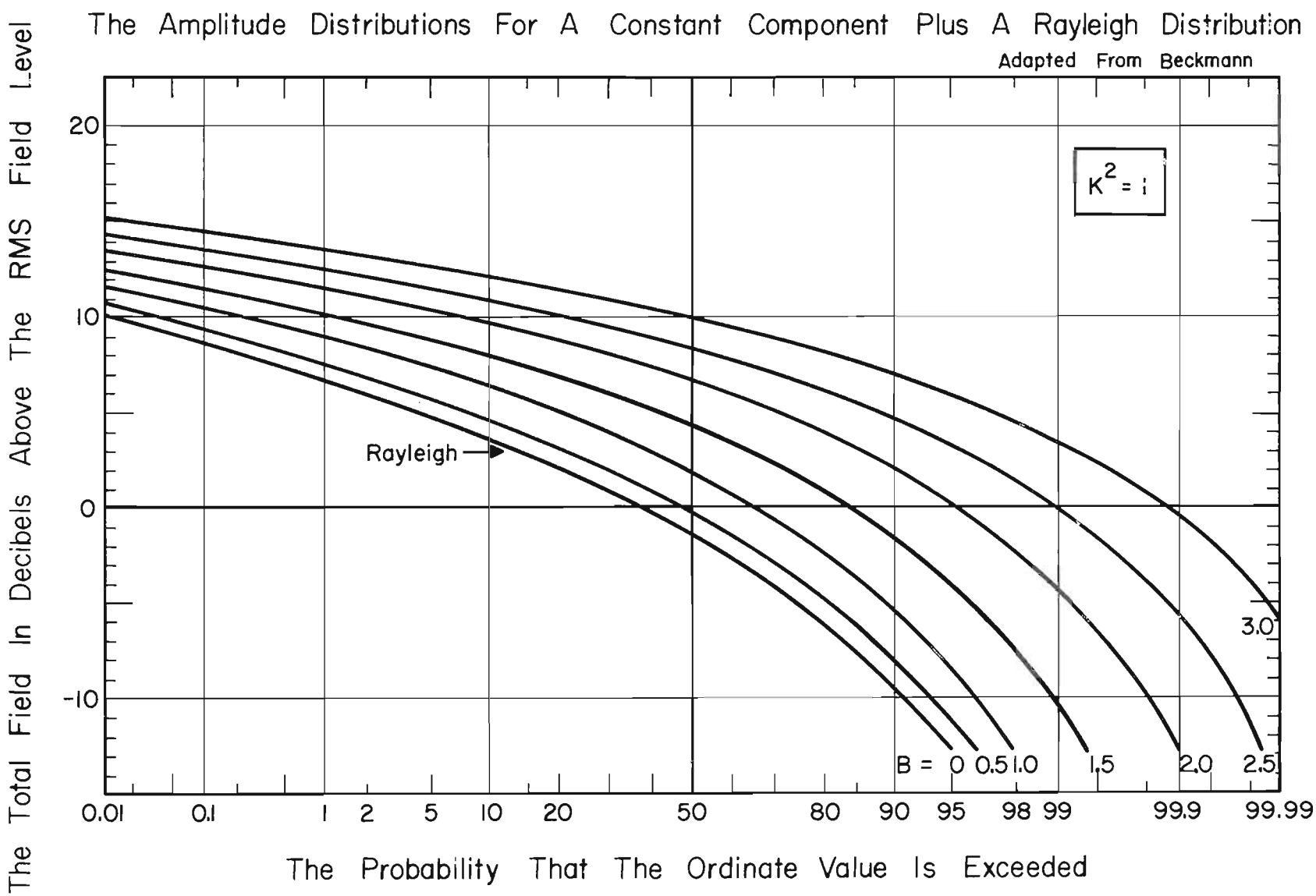
The Amplitude Distributions For A Constant Component Plus A Rayleigh Distribution
Adapted From Beckmann
The Total Field In Decibels Above The RMS Field Level
20
10
0
-10
$K^2 = 1$
Rayleigh
B = 0 0.5 1.0 1.5 2.0 2.5 3.0
0.01 0.1 1 2 5 10 20 50 80 90 95 98 99 99.9 99.99
The Probability That The Ordinate Value Is Exceeded

Figure 15a

The ratio of the constant component (the direct field) to the RMS value of the random field is indicated by B on the distribution curves. The parameter K is a measure of the anisotropic scattering of the random components by the terrain. For a very rough reflecting or scattering surface, the phases of the random components are uniformly distributed and K^2 is unity. For less rough surfaces, such as the sea in fair weather or rolling, pastoral terrain, the pattern of roughness differes with direction and K^2 departs from unity. The distribution of the randomly reflected or scattered components may be represented by that for the vector sum of two orthogonal random components--a Hoyt distribution. Each component has an amplitude that is normally distributed about a mean of zero and the K^2 is the ratio of the variances of the two distributions.

If there is no constant (direct field) component, then $B = 0$, and the total field distribution reduces to that for the random components, a Hoyt distribution (Hoyt, 1947; Beckmann, 1964). If in addition, the surface is extremely rough so that K^2 is unity, the distribution reduces to a Rayleigh distribution. See figure 15a with $B = 0$. The distributions of figure 15a for $B > 0$ are known as the Nakagami-Rice distribution (Nakagami, 1964; Rice, 1944 and 1945; Norton et al., 1955; and Burns, 1964).

Note that the sum of a direct field and many randomly reflected components will produce distributions similar to those given by figures 15a through 15e. The distribution, however, merely implies the sum of many random components, one of which is constant and dominant for large values of B. A variety of alternate presentations of the information in figure 15a through 15e is given by Beckmann (1962).

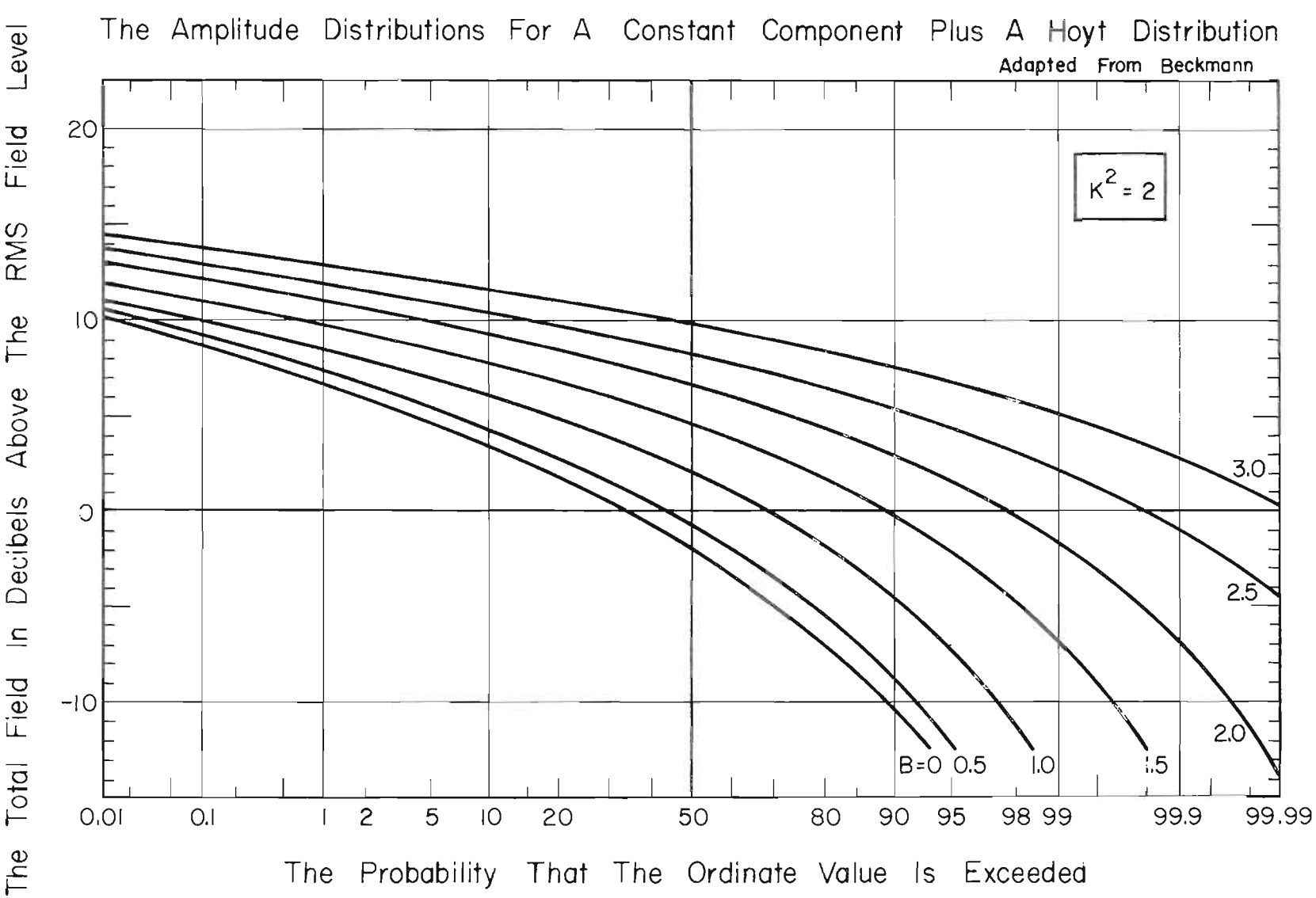
The Amplitude Distributions For A Constant Component Plus A Hoyt Distribution
Adapted From Beckmann
$K^2 = 2$
B=0
0.5
1.0
1.5
2.0
2.5
3.0
20
10
0
-10
0.01
0.1
1
2
5
10
20
50
80
90
95
98
99
99.9
99.99
The Total Field In Decibels Above The RMS Field Level
The Probability That The Ordinate Value Is Exceeded

Figure 15b

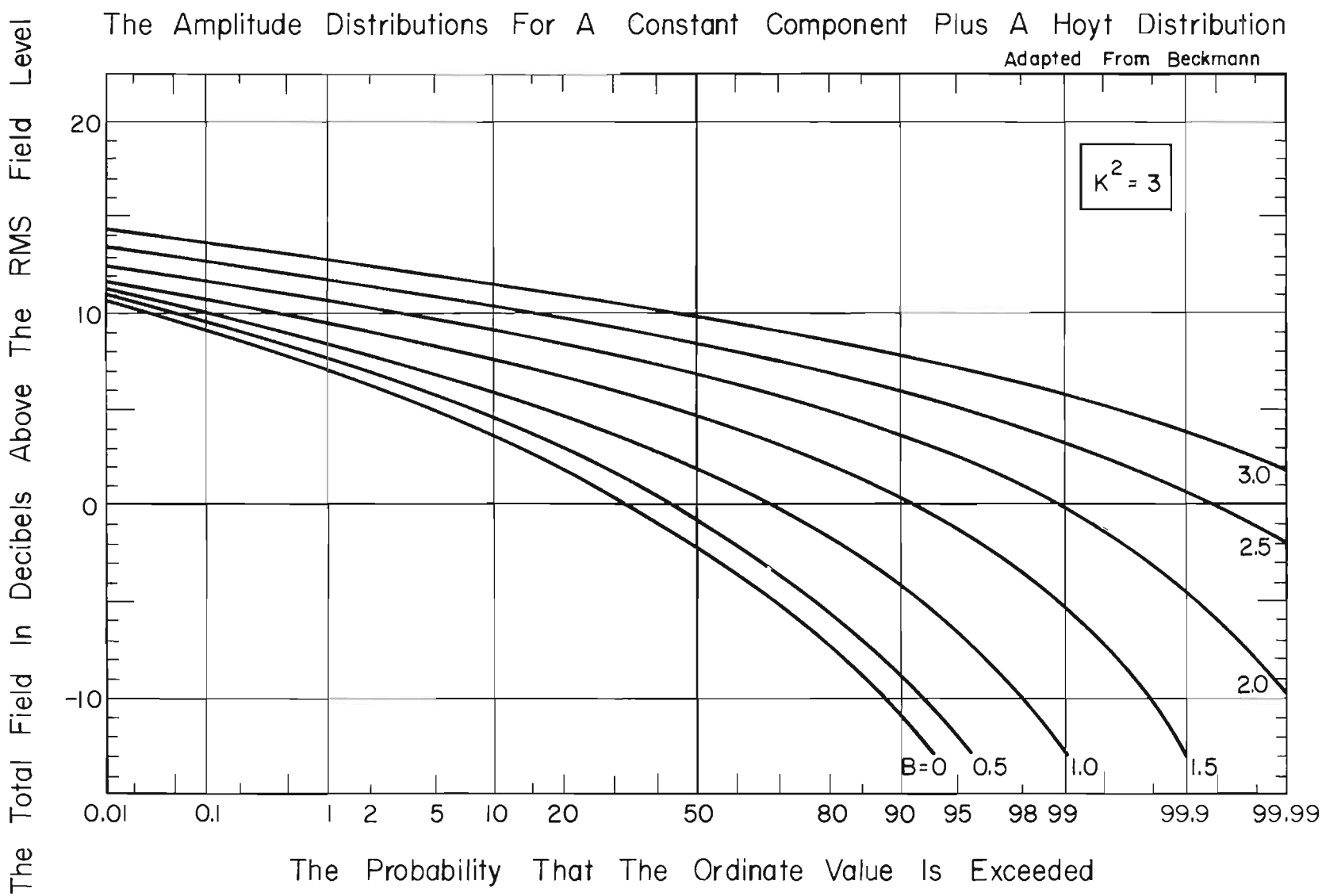
The Amplitude Distributions For A Constant Component Plus A Hoyt Distribution
Adapted From Beckmann
$K^2 = 3$
3.0
2.5
2.0
1.5
1.0
0.5
B=0
20
10
0
-10
0.01
0.1
1
2
5
10
20
50
80
90
95
98
99
99.9
99.99
The Total Field In Decibels Above The RMS Field Level
The Probability That The Ordinate Value Is Exceeded

Figure 15c

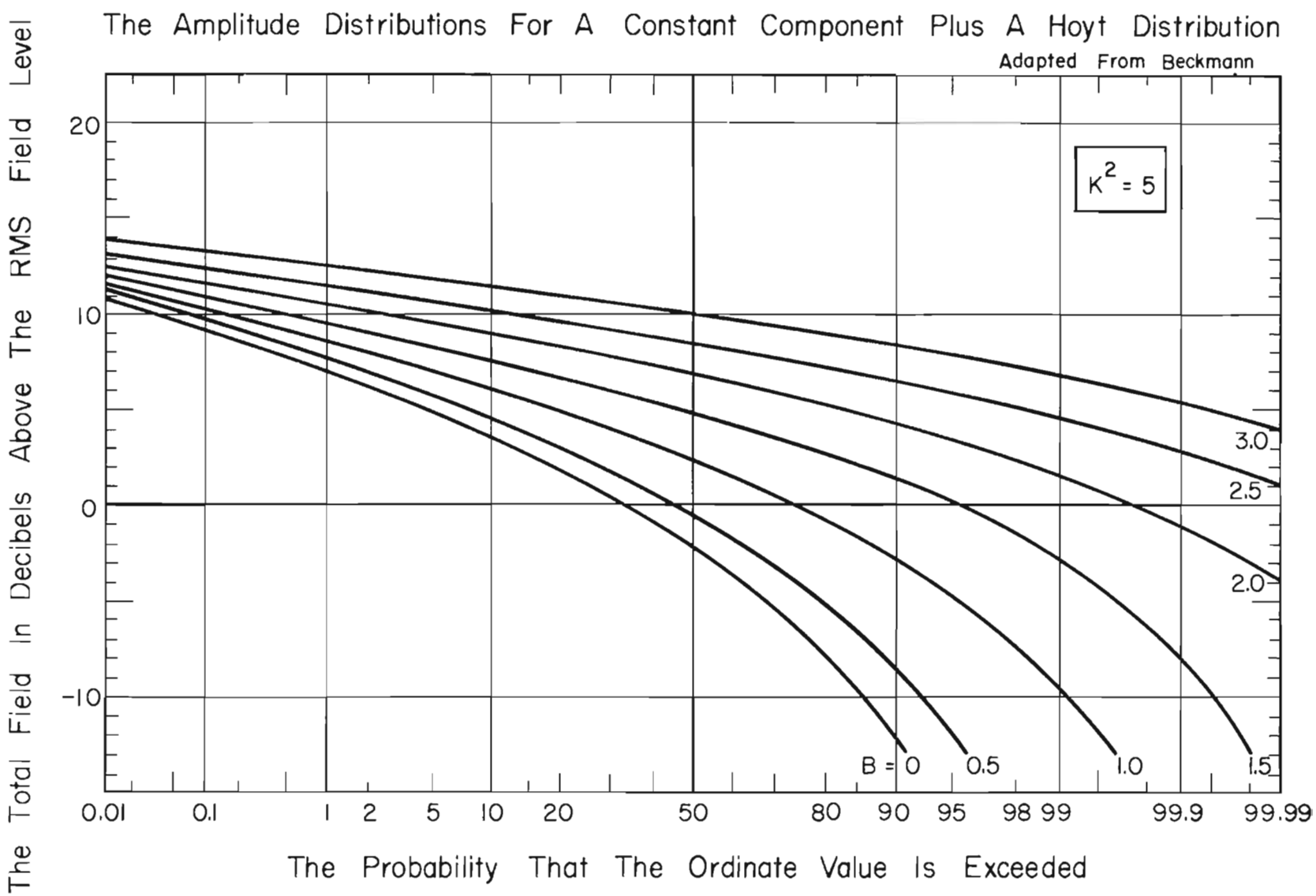
The Amplitude Distributions For A Constant Component Plus A Hoyt Distribution
Adapted From Beckmann
$K^2 = 5$
B = 0
0.5
1.0
1.5
2.0
2.5
3.0
20
10
0
-10
0.01
0.1
1
2
5
10
20
50
80
90
95
98
99
99.9
99.99
The Total Field In Decibels Above The RMS Field Level
The Probability That The Ordinate Value Is Exceeded

Figure 15d

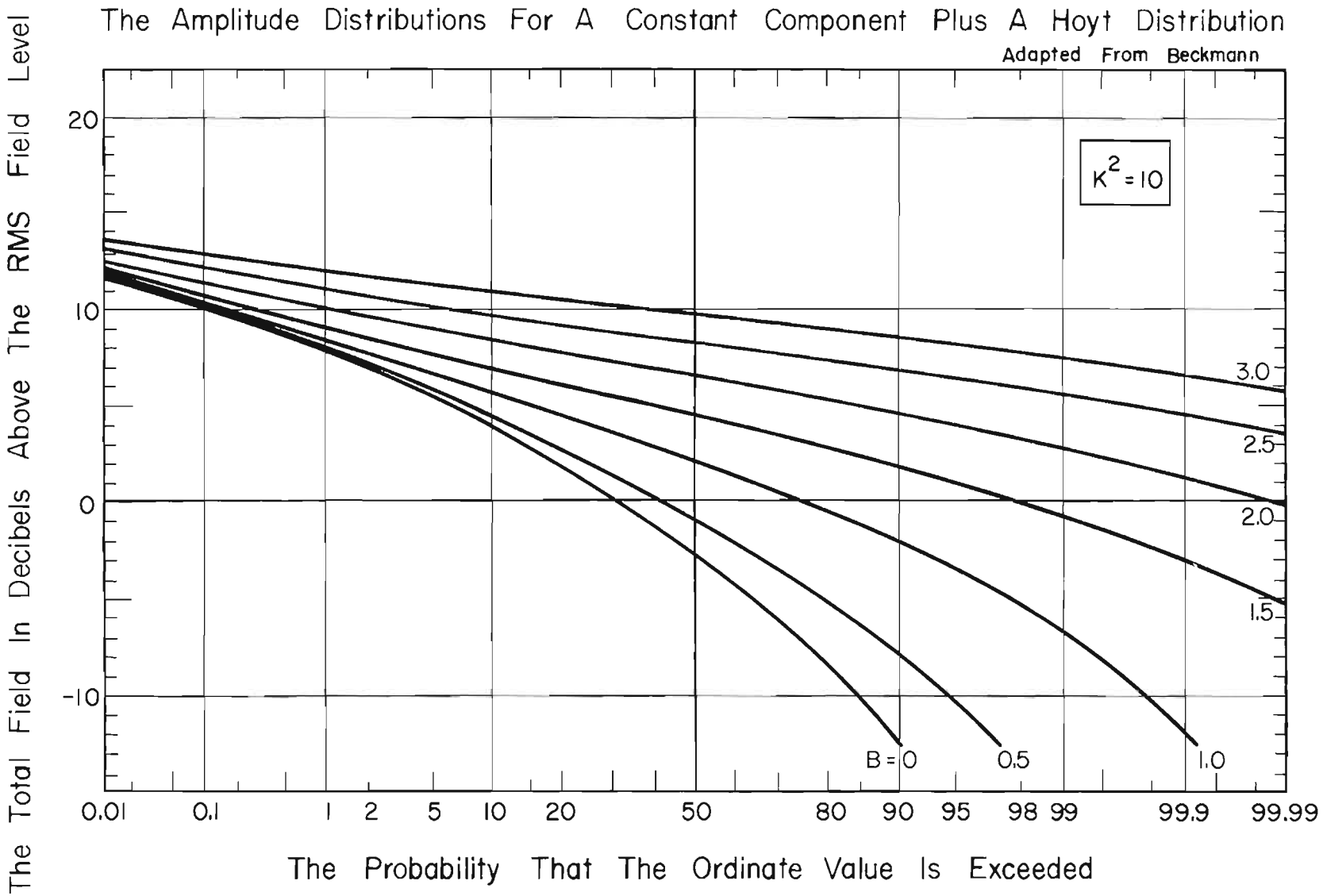
The Amplitude Distributions For A Constant Component Plus A Hoyt Distribution
Adapted From Beckmann
$K^2 = 10$
3.0
2.5
2.0
1.5
1.0
0.5
B = 0
20
10
0
-10
0.01
0.1
1
2
5
10
20
50
80
90
95
98
99
99.9
99.99
The Total Field In Decibels Above The RMS Field Level
The Probability That The Ordinate Value Is Exceeded

Figure 15e

For very small grazing angles the reflected wave is essentially given by the specularly reflected component. The signal distribution caused by interference between the direct wave and this specularly reflected component tends to be steeper than a Rayleigh distribution for strong specular reflection. The resultant two-component multipath distribution is given by figure 16a. Similar theoretical and experimental curves are given by Quarta (1964, 1966). The reflection coefficient is indicated by a and the rms field is therefore $\sqrt{1 + a^2}$ (Dougherty, 1967). The total field is indicated in terms of decibels above this rms value. Again, the distribution does not imply a direct wave plus a specularly reflected component from the terrain; the distribution merely implies two constant components with a uniformly distributed difference in phase. Hence figure 16a, as well as 15a through 15e, describes conditions that may be due to any of the multipath fading mechanisms. Additional information, described in section 6, is usually required to distinguish between some of the multipath mechanisms.

The most general situation, occurring for moderately small angles of incidence, involves two constant components (direct wave plus the specularly reflected wave) and a randomly distributed component (caused by nonspecular reflection and atmospheric scattering). The complete family of distribution curves has not been computed, but an illustrative example is presented in figure 16b (Dougherty, 1967). There, a is as previously defined and the rms random field value is indicated by S in decibels above the two-component rms value, $\sqrt{1 + a^2}$. Again, the total field r is expressed in decibels above the total rms field value $\tilde{r}$.

In some of the foregoing distributions, an a priori determination of the signal distribution from the parameter value depends upon an estimate of the mean power in the random component. In the case of terrain reflections, an estimate is obtainable from the distribution and

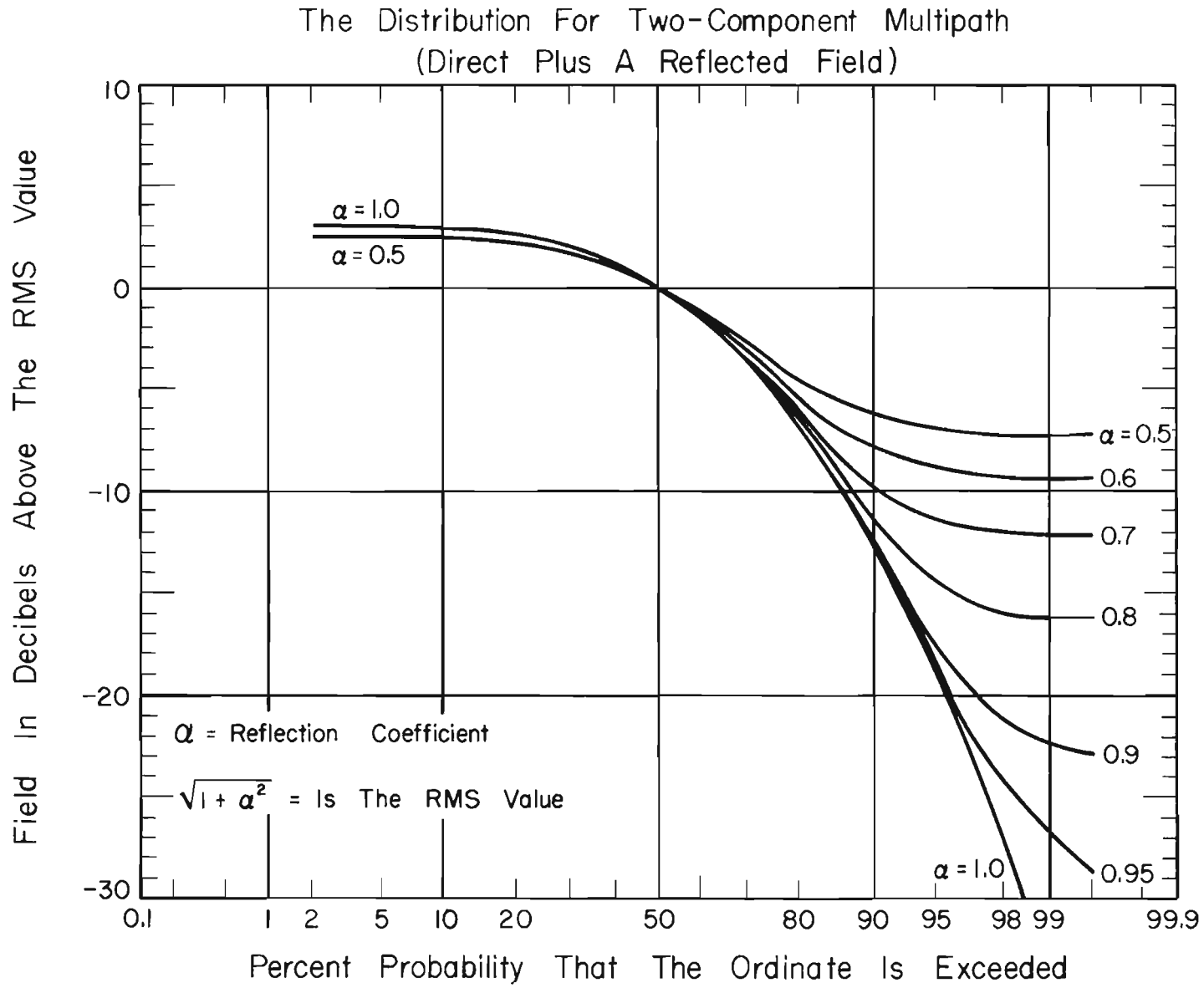
The Distribution For Two-Component Multipath
(Direct Plus A Reflected Field)
Field In Decibels Above The RMS Value
10
0
-10
-20
-30
α = 1.0
α = 0.5
α = 0.5
0.6
0.7
0.8
0.9
0.95
α = 1.0
α = Reflection Coefficient
√1 + α² = Is The RMS Value
0.1
1
2
5
10
20
50
80
90
95
98
99
99.9
Percent Probability That The Ordinate Is Exceeded

Figure 16a

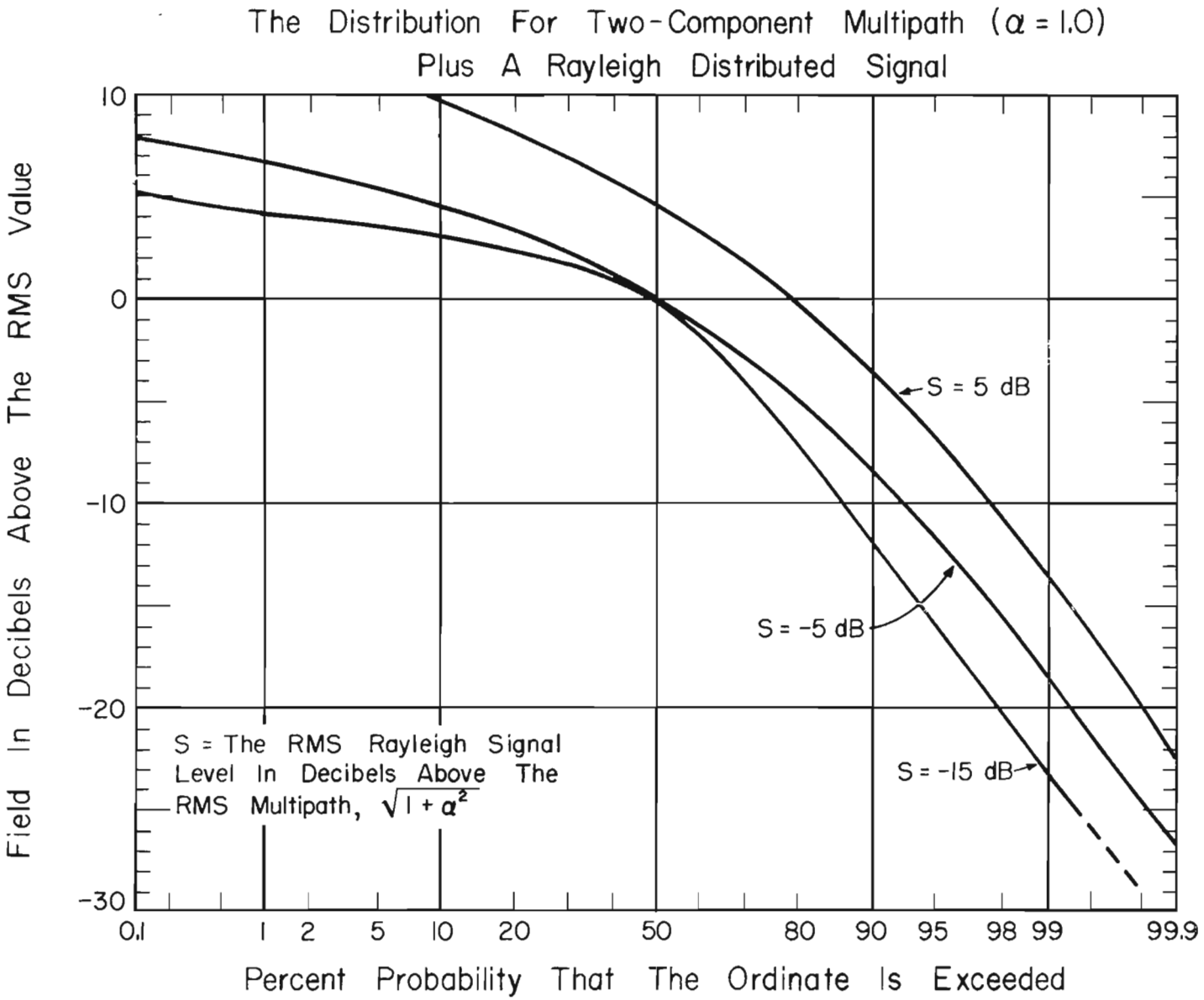
The Distribution For Two-Component Multipath (α = 1.0)
Plus A Rayleigh Distributed Signal
Field In Decibels Above The RMS Value
10
0
-10
-20
-30
S = 5 dB
S = -5 dB
S = -15 dB
S = The RMS Rayleigh Signal Level In Decibels Above The RMS Multipath, $\sqrt{1+\alpha^2}$
0.1
1
2
5
10
20
50
80
90
95
98
99
99.9
Percent Probability That The Ordinate Is Exceeded

Figure 16b

correlation function of the terrain irregularities (Beckmann and Spizzichino, 1963). However, these are also often unknown. Frequently, a knowledge of the parameters is not necessary; it is usually sufficient to know which family of distributions is expected. Alternately, one is interested in comparing observed distributions with those of figure 15a through 16b, to obtain an estimate of the likely fading mechanisms.

5. PROTECTION AGAINST MULTIPATH FADING

Diversity reception is the most generally successful technique for reducing the microwave fading caused by multipath (Murray and Flager, 1965). Diversity techniques may be either redundant or non-redundant. Redundant techniques include two or more transmission channels carrying the same information either at the same time (frequency diversity) or with a delay time between the channels (time diversity). Nonredundant techniques include two or more propagation paths accomplished either by spaced antennas (space diversity) or by alternate multilink routes (route diversity). Here we examine both the frequency and space diversity techniques.

Frequency and space diversity are physically different techniques whose theoretical advantages depend upon the specific application and the type of optimization required. As a practical matter, space diversity appears preferable because frequency diversity possesses no known inherent advantage sufficient to offset its contribution to the serious problem of frequency allocation in a crowded spectrum. Nevertheless, design procedures for both diversity techniques are given below. They determine the separation (frequency or spatial) that provides protection against multipath fading of more than $\hat{A}$ dB below the free space field.

For any given propagation path, one could treat the rough terrain between the terminal antennas as a randomly distributed variable, and obtain, by the least-squares method, a standard deviation for the terrain relative to a median spherical surface. Such a procedure would determine a curve, such as in figure 12, and therefore the range of gradients over which protection would be required. This may, of course, vary with the season because of crop cover, snow, etc. An alternative approach avoids the least-squares analysis of uniformly rough terrain by assuming that severe fading could occur (components of equal amplitude) for any value of the refractive index gradient. The significant range of gradients is then determined in terms of the percent of hours that protection is required. For example, assuming that figure 3 is applicable and the terminal antennas are of sufficient height to avoid excessive diffraction fading, one finds the critical range (for protection against multipath fading during 99.95 percent of the hours) extends out to -430 N units/km or a k value of -0.575. A diversity separation in frequency or space is chosen so that the fading will not exceed $\hat{A}$ for the given range of refractive index gradients. The following paragraphs outline the applicable design procedures.

5.1. Separations for Frequency Diversity

The design procedures for frequency diversity separations depend upon whether the multipath mechanism is that shown by the top or bottom drawing in figure 5; i.e., whether the second ray path is due to a specular reflection or simply due to refraction phenomena. For multipath involving reflection, the interference field, E, is related to the free space field, E_0, by

$$|E/E_0|_s = |2 \sin \nu(k)\pi|, \qquad (9a)$$

$$A_s = -20 \log |E/E_0|_s \text{ dB} \quad , \tag{9b}$$

$$\nu(k) = \phi(k)/2\pi \quad , \tag{9c}$$

where $\phi(k)$ is the phase difference in radians for the path length difference between the two field components here assumed to be equal. The subscript, s for sine, is used to identify a quantity for multipath due to specular ground reflection. Equation (9a) includes the effect of the phase shift caused by reflection. This phase shift closely approximates π radians for the small grazing angles normally encountered on microwave line-of-sight paths. The corresponding expressions for multipath due only to refraction (subscript c for cosine) are

$$|E/E_0|_c = |2 \cos \nu(k) \pi| \quad , \tag{10a}$$

$$A_c = -20 \log |E/E_0|_c \quad . \tag{10b}$$

For protection against multipath fading of more than $\hat{A}$ dB below the free space field, a useful parameter is Δ, defined by

$$\hat{A} = -20 \log |2 \sin \Delta\pi| \text{ dB} \quad . \tag{11}$$

For a nondiversity transmission frequency, the multipath-received signal attenuation relative to free space is $A(f_1, k)$. A second transmission frequency, f_2, which is separated to achieve diversity, will have a multipath signal attenuation given by $A(f_2, k)$. The separation $f_2 - f_1$ is then chosen to insure either $A(f_1, k)$ or $A(f_2, k)$ will be less than or equal to $\hat{A}$ at any instant. The minimum separation to accomplish this, for multipath fading associated with reflection or refraction, respectively, is given by

$$\left(\frac{f_2-f_1}{f_1}\right)_s = \frac{2\Delta}{1-\Delta} \qquad (12a)$$

$$\left(\frac{f_2-f_1}{f_1}\right)_c = \frac{4\Delta}{1-2\Delta} \qquad (12b)$$

for $f_2 > f_1$.

The maximum attenuation $\hat{A}$ will occur, for these expressions, near the first null; for path length differences $\nu(k)$ near 1.0 and 0.5, respectively. These expressions were derived with the aid of the diagram of figure 17 and are plotted versus $\hat{A}$ in figure 18. In figure 18 the reflection coefficient, a, as mentioned previously, has been taken as unity. For the effect of $a < 1.0$ see Dougherty (1967). If N is the largest integral value of $\nu(k)$ expected for the critical range of gradients, then a "maximum" separation may be determined from

$$\left(\frac{f_2-f_1}{f_1}\right)_s = \frac{2\Delta}{N-\Delta} \qquad (13a)$$

$$\left(\frac{f_2-f_1}{f_1}\right)_c = \frac{4\Delta}{2N-1-2\Delta} \quad , \qquad (13b)$$

for $f_2 > f_1$. For $f_2 < f_1$, the corresponding expressions may be obtained from (12a) through (13b) by replacing Δ by $-\Delta$.

There are actually several "minimum" and "maximum" separations, ranges of frequency separations, over which the protection $\hat{A}$ is achieved. Some of these additional ranges are constructed in figure 19. For an alternate description of these ranges of frequency separation and description of optimum frequency separations see the CCIR Doc. (1965) for multipath due to reflection and Magnuski (1956) for multipath due to refraction.

DIAGRAM FOR DERIVING THE MINIMUM FREQUENCY DIVERSITY SEPARATIONS

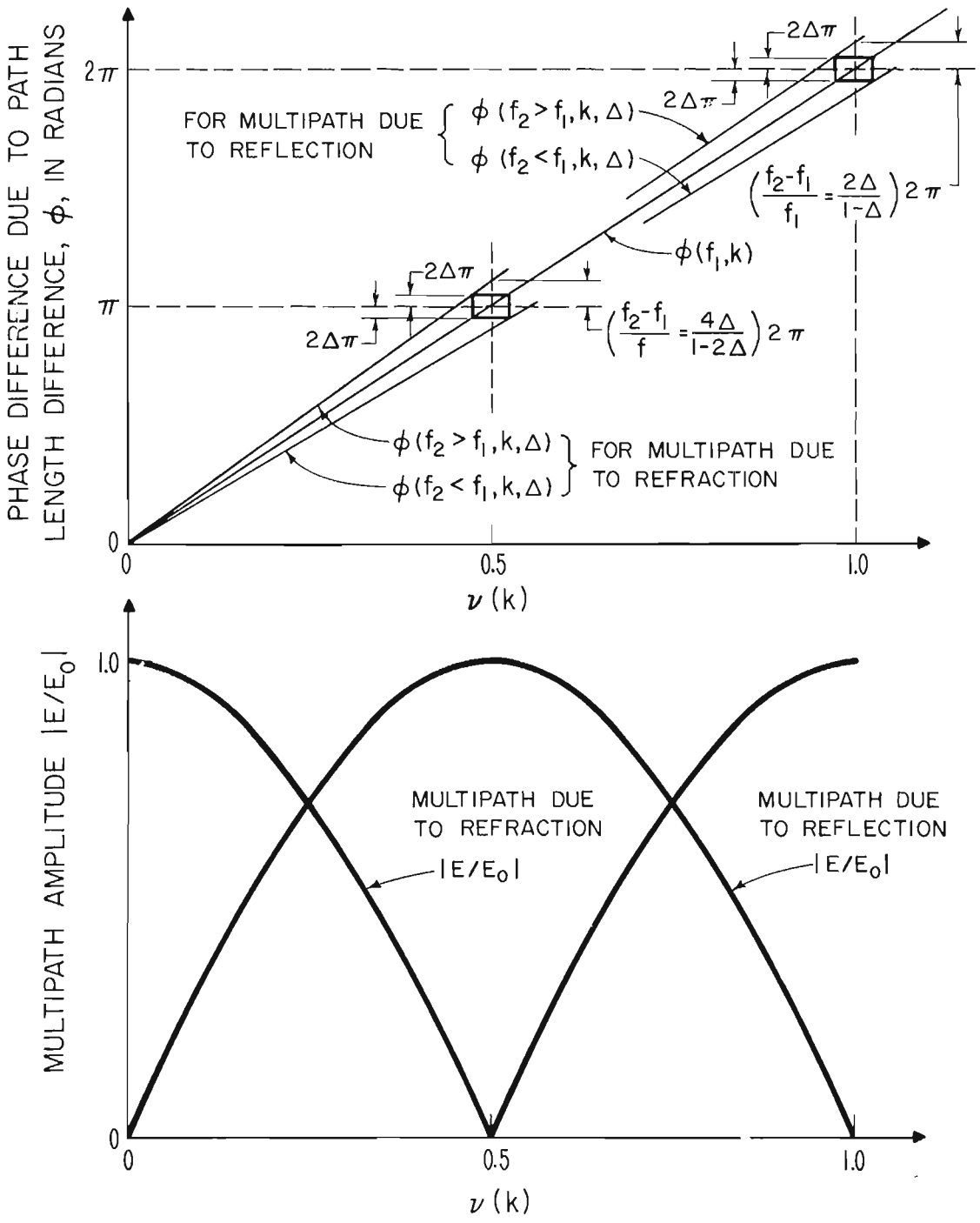

Figure 17

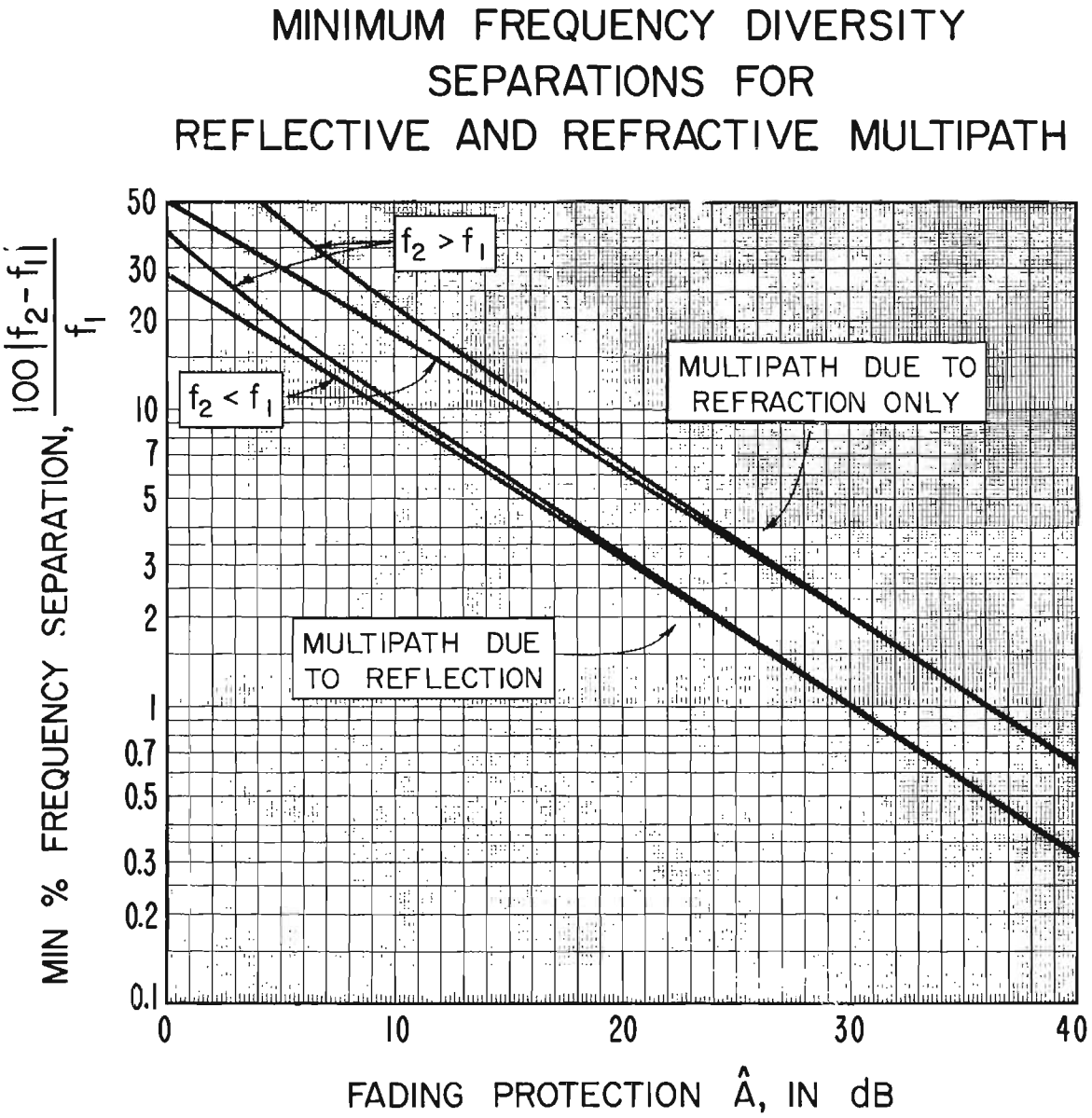
MINIMUM FREQUENCY DIVERSITY
SEPARATIONS FOR
REFLECTIVE AND REFRACTIVE MULTIPATH
MIN % FREQUENCY SEPARATION, 100|f2-f1| / f1
50
30
20
10
7
5
3
2
1
0.7
0.5
0.3
0.2
0.1
f2 > f1
f2 < f1
MULTIPATH DUE TO
REFRACTION ONLY
MULTIPATH DUE
TO REFLECTION
0
10
20
30
40
FADING PROTECTION Â, IN dB

Figure 18

GRAPHICAL LOCATION OF SOME OF THE PERMISSIBLE AND FORBIDDEN
FREQUENCY SEPARATIONS FOR A SPECIFIED PROTECTION AGAINST MULTIPATH FADING

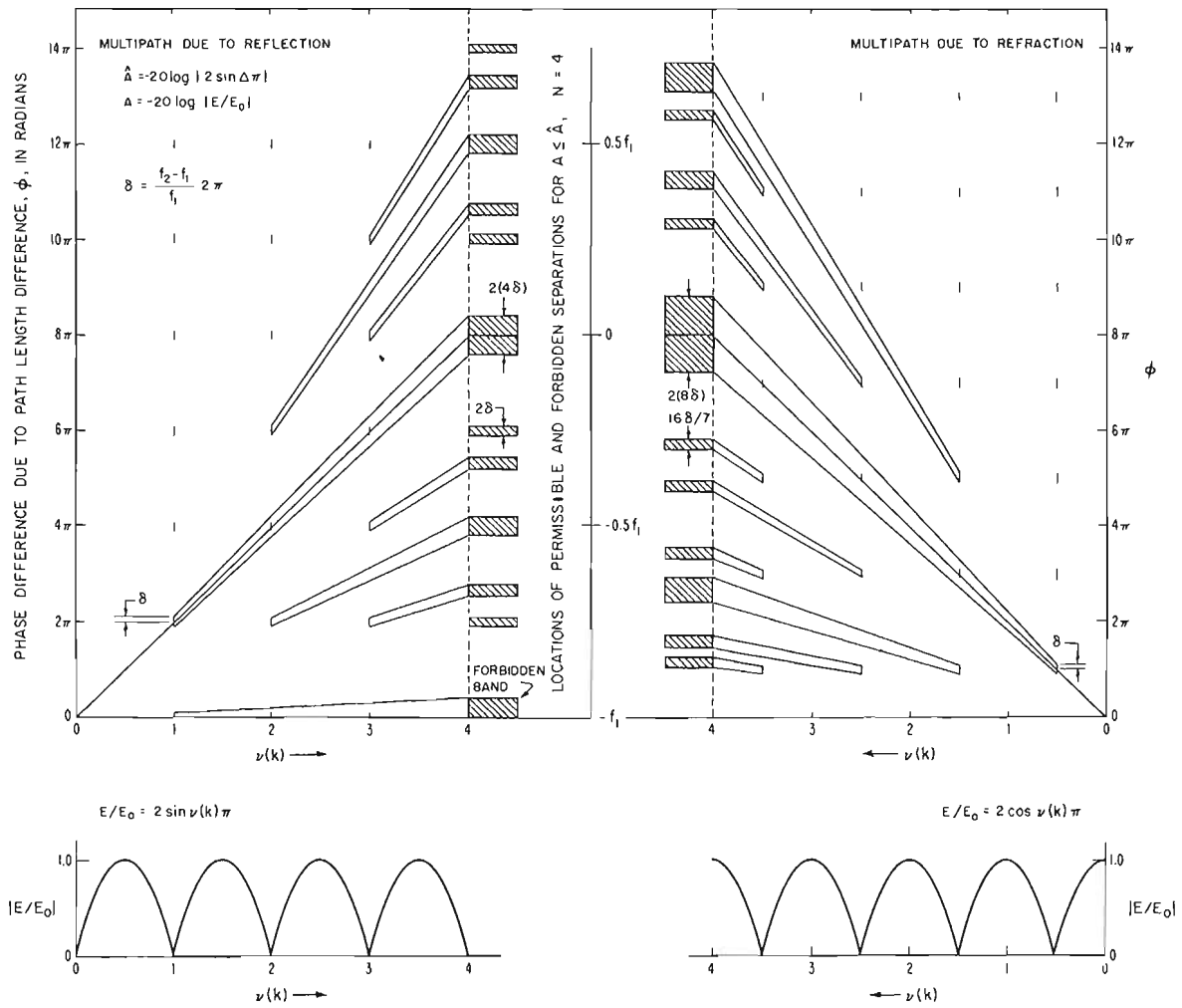

Figure 19

To illustrate the interference pattern for multipath for specular reflection, we plot (9a) in figure 20 for a propagation path near Cape Kennedy, Florida, whose frequency separation closely approximates the minimum (12a) required for protection corresponding to $\hat{A}$ = 20 dB. The maximum attenuation experienced near $\nu_1 = 1$ will occur again for the integral values of ν closest to $(1 - 2\Delta)/2\Delta$, which may be deduced from figure 19. By adding 0.5 to the ν scales of figure 20, we use the curves to depict (10a) for the minimum separation (12b) corresponding approximately to $\hat{A}$ = 26 dB. The percent time scale would not, however, be applicable.

5.2. Multipath Parameters

To determine N in (13a) or (13b) we must determine the phase lag for the path length difference between the direct ray and a ground reflected ray. This same phase is required for the space diversity design. The path length difference is readily determined by iterative procedures or nomographs (Beckmann and Spizzichino, 1963). Some simplification is achieved by using normalized parameters (CCIR Doc. 1965) and graphs.

For space diversity reception, it is convenient to normalize antenna heights to the antenna height at the transmitting end of the path, h_0, as shown in figure 21a. The non-diversity antenna height h_1 and the diversity-spaced antenna height h_2 are normalized by

$$\eta_i = h_i/h_0, \quad i = 1, 2 \quad . \tag{14}$$

For phase lag due to path length difference, a convenient reference value is that for symmetrical geometry ($h_1 = h_0$) and a flat ($k = \infty$) earth:

$$\nu_0 = \nu(h_1 = h_0, k = \infty) = 0.006673\, h_0^2\, f/d_0 \quad , \tag{15}$$

ILLUSTRATIVE INTERFERENCE PATTERN FOR MULTIPATH FADING
DUE TO SPECULAR GROUND REFLECTION
AND THE MINIMUM FREQUENCY DIVERSITY FOR PROTECTION TO 20 dB

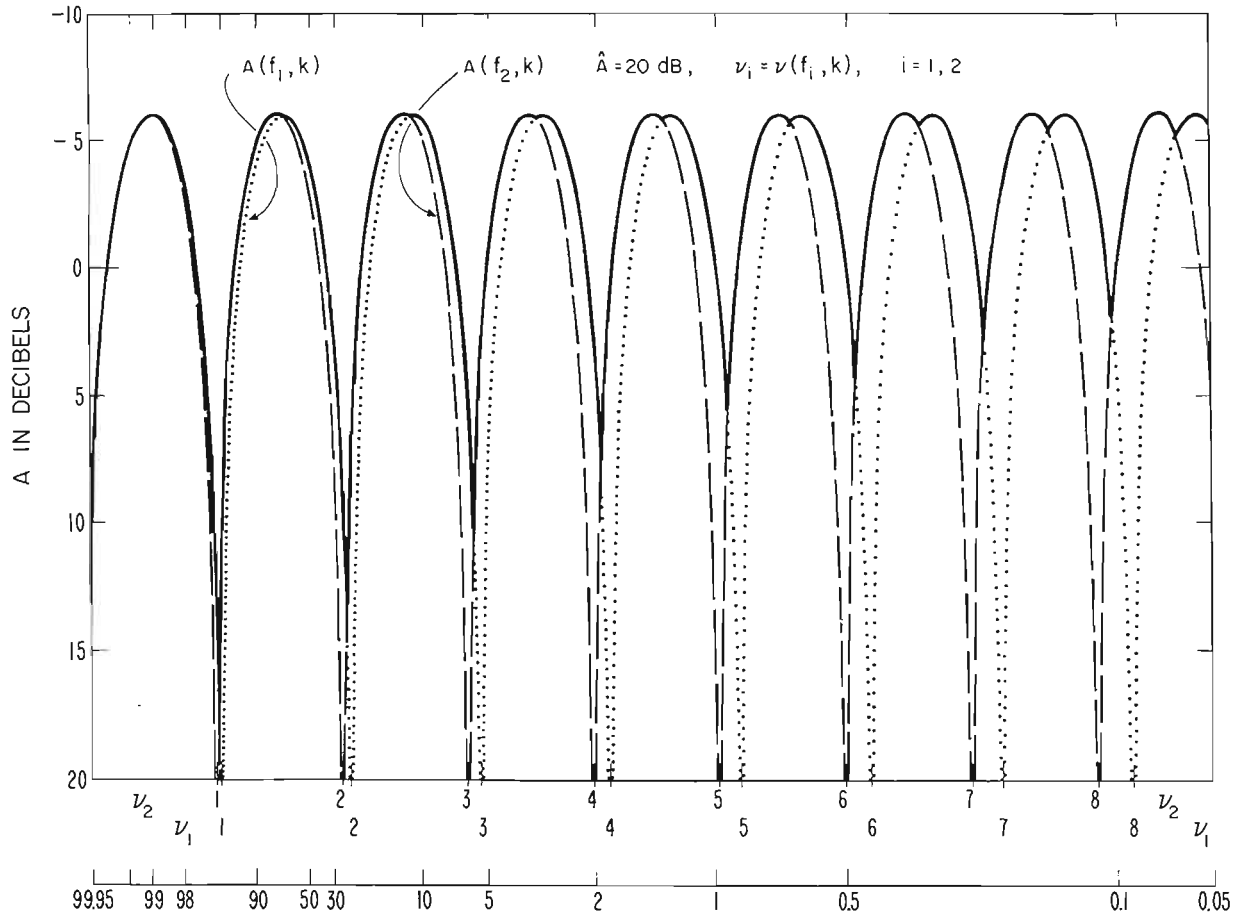

Figure 20

THE NORMALIZED RELATIONSHIP BETWEEN PATH LENGTH DIFFERENCE AND EFFECTIVE EARTH CURVATURE

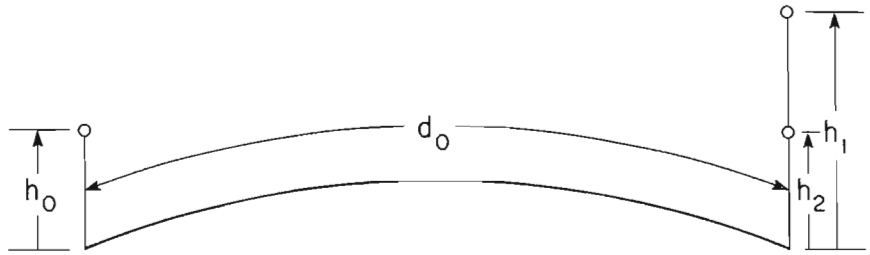

h_0 = THE REFERENCE TERMINAL ANTENNA HEIGHT IN METERS

h_1, h_2 = THE NON-DIVERSITY AND DIVERSITY-SPACED ANTENNA HEIGHTS IN METERS

d_0 = THE TOTAL PATH LENGTH IN KILOMETERS

f = THE TRANSMISSION FREQUENCY IN GIGAHERTZ

k = THE EFFECTIVE EARTH RADIUS FACTOR

ϕ = THE PHASE DIFFERENCE DUE TO PATH LENGTH DIFFERENCE

$$\eta_i = h_i / h_0, \quad i = 1, 2 \qquad\qquad g = \nu / \nu_0$$

$$\nu_0 = 6.6732\ 10^{-3} h_0^2 f / d_0 \qquad\qquad \nu = \phi / 2\pi$$

$$\mu = 0.07849\ d_0^2 / k h_0$$

Figure 21a

where the reference antenna height h_0 is in meters, the transmission frequency f_1 is in gigahertz, and the total path length d_0 is in kilometers. The normalized phase difference for a curved earth is then:

$$g(h_i, k) = \nu(h_i, k)/\nu_0 \ . \tag{16}$$

For the effective earth curvature factor, 1/k, a convenient reference value is that for which a symmetrical path ($h_1 = h_0$) would be just grazing. The normalized effective earth curvature factor is therefore

$$\mu = 0.07849\ d_0^2/kh_0 \ , \tag{17}$$

where the units are as specified for (15). Graphs of g versus μ are shown in figures 21b and 21c for various values of η. The ranges of g and μ are chosen to be representative of those most commonly encountered. Generally $\mu > -4$ for those paths with terminal antenna heights sufficiently large to avoid diffraction fading. If $\mu < -4$, then g may no longer be single-valued; and propagation may occur over an effective earth sufficiently concave to involve more than one reflected ray path (Furutsu, 1965). There is a relation between the family of g versus μ curves for $\eta > 1.0$ and those for $\eta < 1.0$. For example if,from figure 21b, we determine a value g_1, for given η_1, μ_1, and ν_{01} values, then $\nu_1 = g$, and ν_{01} may also be determined from $\eta' = 1/\eta_1$, $\mu' = \mu_1/\eta_1$, $\nu_0' = \eta_1^2 \nu_{01}$. Thus $\eta_1 = 0.5$, $\mu_1 = -1.0$, and $\nu_{01} = 2$ determines $g_1 = 0.875$ from figure 21b so that $\nu_1 = g_1 \nu_{01} = 1.75$. Similarly $\eta' = 2$, $\mu' = -2$, and $\nu_0' = 0.5$ determines $g' = 3.5$ from figure 21b so that $\nu' = g'\nu_0' \approx 1.7$. For $\eta \geq 20$, $g \approx \eta - \mu$.

To illustrate the application of (14) through (17) we determine the N of (13a and b) for the minimum k value, -0.575,of section 5. For a transmission frequency of f = 8 GHz over a path of length d = 25 km with terminal antenna heights, $h_0 = 39$ m and $h_1 = 25$ m, (14) yields $\eta_1 = 0.641$. Then (15) gives $\nu_0 = 3.248$ and (17) yields $\mu(k = -0.575) = -2.188$. From figure 21b, $g_1 = 1.75$, so that (16) gives $\nu_1 = 5.684$, and then N = 5.0.

THE NORMALIZED RELATIONSHIP BETWEEN PATH LENGTH DIFFERENCE AND EFFECTIVE EARTH CURVATURE

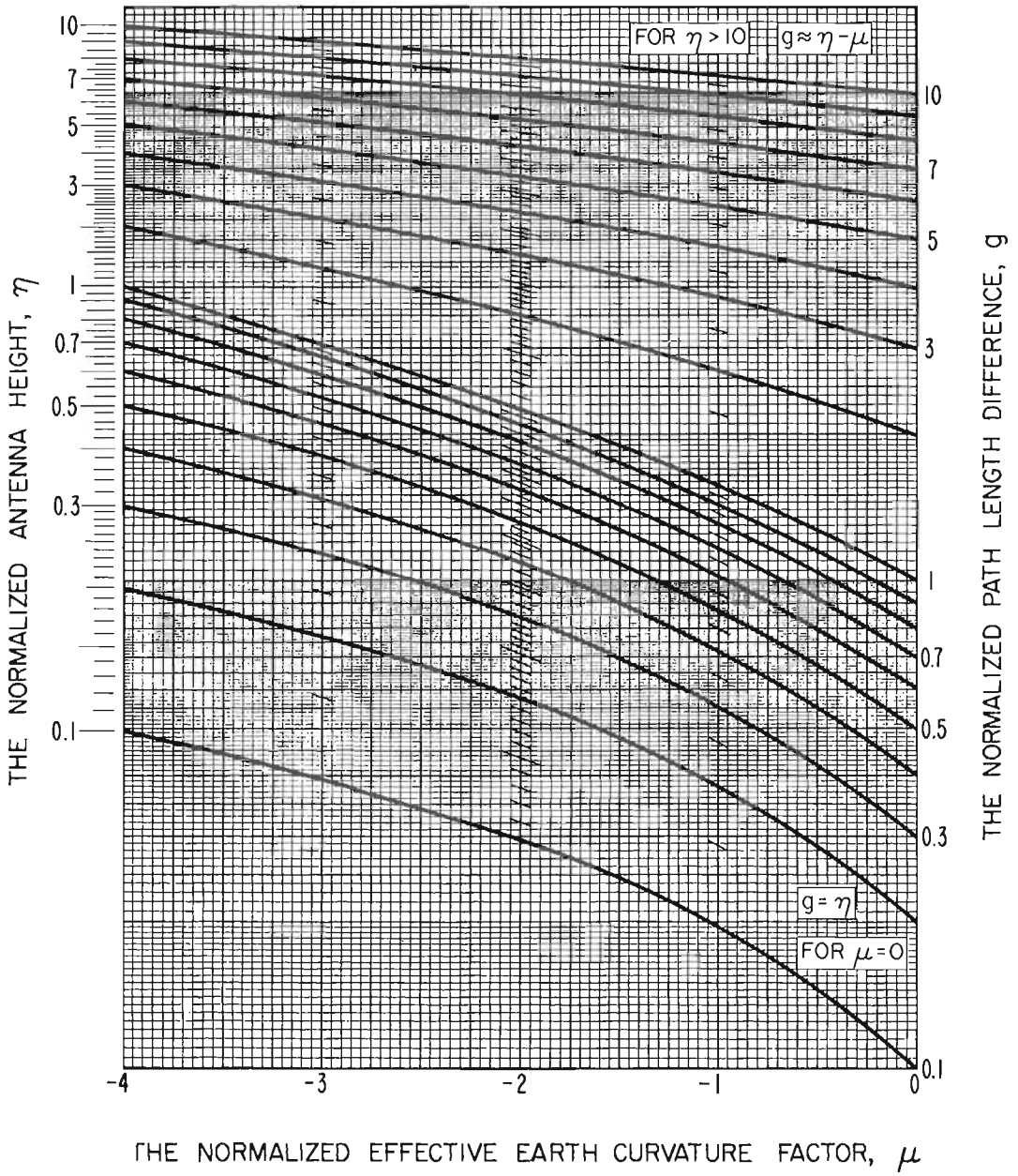

Figure 21b

THE NORMALIZED RELATIONSHIP BETWEEN PATH LENGTH DIFFERENCE AND EFFECTIVE EARTH CURVATURE

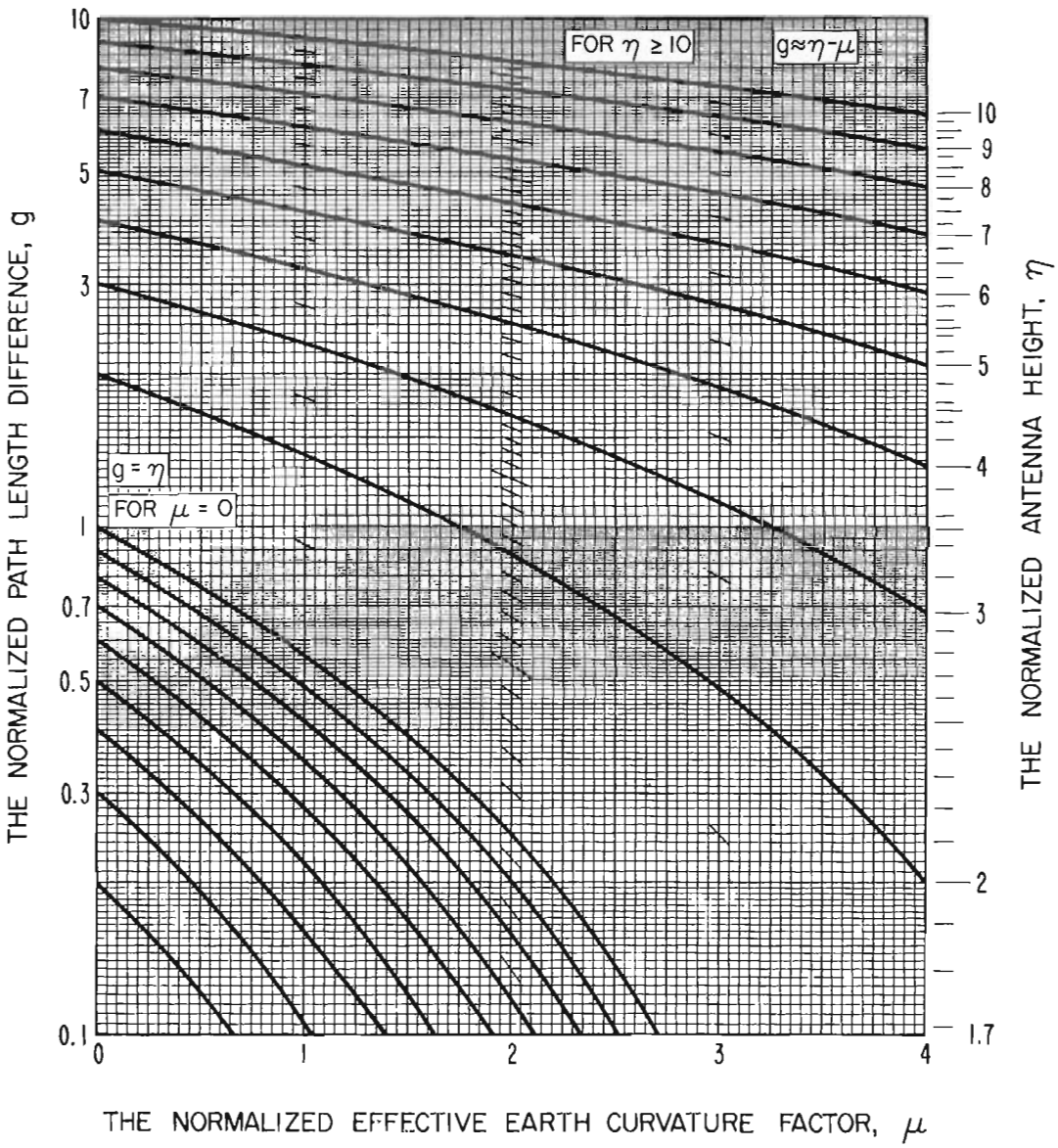

Figure 21c

AN ILLUSTRATION OF
SPACE AND FREQUENCY DIVERSITY DEPENDENCE
UPON PATH LENGTH DIFFERENCE

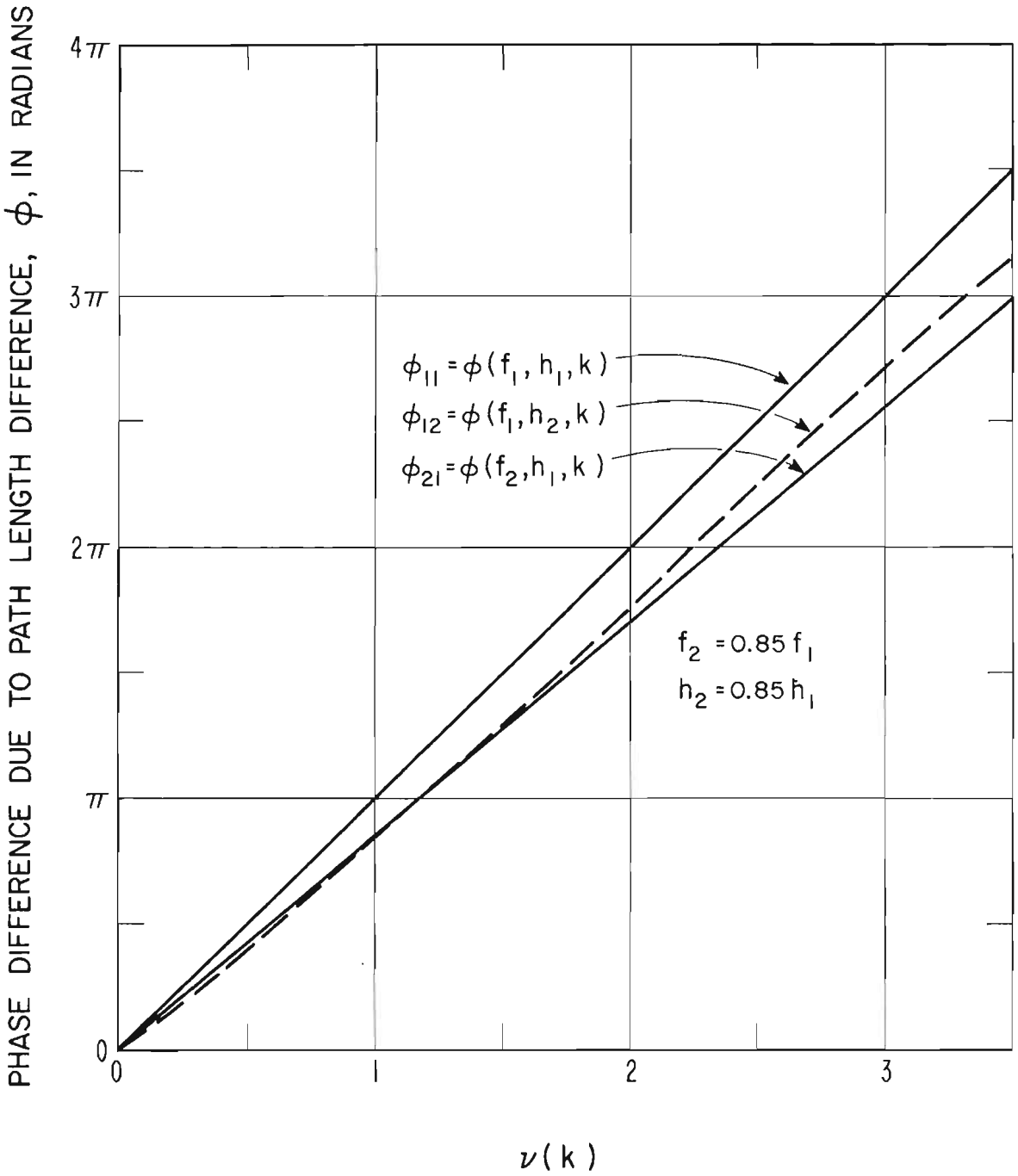

Figure 22

5.3. Separations for Space Diversity

There are similarities in the design considerations for frequency and space diversity. Figure 22 illustrates this. However, the design procedures for space diversity are more complex than those for frequency diversity. This is because the path length difference, proportional to frequency, is not as simply related to antenna height, and this is demonstrated by the difference in the shape of the diversity-separation curves $\phi_{21} = \phi(f_2, h_1, k)$ and $\phi_{12} = \phi(f_1, h_2, k)$ in figure 22. The curve ϕ_{11} of figure 22 was obtained by rectification of the $\eta = 1.0$ curve of figure 21, and the ϕ_{12} curve is that resulting for $\eta = 0.85$.

For multipath due to reflection, the minimum separation $(\eta_1 - \eta_{2\,max})$ for space diversity is determined by means of the equations that apply near the first field null:

$$1 + \Delta = \nu(h_1, k_{1\Delta}) = \nu_0 g(\eta_1, \mu_{1\Delta}) \qquad (18a)$$

$$1 - \Delta = \nu(h_2, k_{1\Delta}) = \nu_0 g(\eta_2, \mu_{1\Delta}) \quad , \qquad (18b)$$

for $h_2 < h_1$. These may be derived with the aid of figure 22. For a given protection $\hat{A}$, Δ is specified by (11). Since ν_0 is obtained from (15) for the given path parameters (antenna heights h_0 and h_1 are specified for the diffraction fading protection), $g(\eta_1, \mu_{1\Delta})$ is determined by (18a). For η_1 and $g(\eta_1, \mu_{1\Delta})$, figures 21b or 21c will yield $\mu_{1\Delta}$. Again, Δ, ν_0 will determine $g(\eta_1, \mu_{1\Delta})$ from (18b). This $g(\eta_2, \mu_{1\Delta})$ and the $\mu_{1\Delta}$, just determined, will determine η_2 (see figs. 21b or 21c).

Similarly the first "maximum" spatial separation $(\eta_1 - \eta_{2\,min})$ is determined by the equations

$$N - \Delta = \nu(h_1, k_{N\Delta}) = \nu_0 g(\eta_1, \mu_{N\Delta}) \qquad (19a)$$

$$N - 1 + \Delta = \nu(h_2, k_{N\Delta}) = \nu_0 g(\eta_2, \mu_{N\Delta}) \quad , \qquad (19b)$$

for $h_2 < h_1$. As previously, N is the integral part of ν determined for the minimum expected value of k for the time dependency specified; the k = -0.575 of section 5, for example. For $h_2 < h_1$, replace Δ by $-\Delta$ in (18a) through (19b).

The application of the above is illustrated for the path parameters used in section 5.2, where $\eta_1 = 0.641$ and $\nu_0 = 3.248$. For $\hat{A}$ = 20 dB, $\Lambda = 0.015922$ so that (18a) yields $g(0.641, \mu_{1\Lambda}) = 0.3128$ (fig. 21b), and $\mu_{1\Delta} = 1.0$. Then (18b) yields $g(\eta_2, 1.0) = 0.303$ and therefore $\eta_{max} = 0.621$. Since N = 5, (19a) yields $g(\eta_1, \mu_{N\Lambda}) = 1.534$ and figure 21b gives $\mu_{N\Lambda} = -1.81$. Equation (19b) yields $g(\eta_2, -1.81) = 1.236$, and we obtain (fig. 21b) $\eta_{2\,min} = 0.455$. The first forbidden band is therefore from $\eta = 1.0$ to 0.9688 (0.621/0.641); 0.25 to 24.2 m. The first permissible band is from $\eta = 0.9688$ to 0.71 (0.455/0.641) or 37.8 to 27.7 m.

Additional forbidden bands may be determined in a manner suggested by figure 19. For example, the combination $1 \pm \Delta$ for the left side of (18a) in conjunction with $N \pm \Delta$ for the left side of (18b) will determine additional forbidden bands. The N = 1, 2, are integral values of ν.

6. FADING REMEDIES AS MEASUREMENT TECHNIQUES

Up to this point attention has been directed to the effect of meteorological conditions upon the reception of radio waves. For example, a refractive index profile may be described as applicable to the region between two radio propagation terminals and the possible mechanisms of propagation are then considered. When the spatial relations are proper (perhaps in terms of transmission wavelength), there is an associated fading mechanism and fading occurs in a specific pattern. Thus a fading mechanism may be said to have at least four constituents: (a) the meteorological situation; (b) the propagation path geometry; (c) the transmission frequency; and (d) the resulting fading pattern or characteristics of the received transmission. To this may be added a fifth, the fading remedy. These five components are related, so that given any four one can, at least in principle, deduce something about the remaining constituent.

6.1. Diffraction Fading as a Measurement Technique

To the extent that the foregoing is feasible, a fading situation will permit the indirect measurement of pertinent aspects of the meteorological situation upon successful application of the remedy and measurement of the received field. For example, consider a tropospheric propagation path, nominally line-of-sight, which experiences appreciable attenuation persisting during certain portions of most days. Further, let this fading, characterized by a slight frequency dependency, etc.,be consistent with a diagnosis of diffraction fading. In addition, let application of the appropriate remedy (raising one or both antennas) be effective in reducing the fading or attenuation by approximately the predicted amount. By assuming horizontal stratification of the atmosphere, we can use the available methods of predicting diffraction loss (Bremmer, 1949; Dougherty and Maloney, 1964; Vogler, 1964; Rice et al., 1966; Dougherty and Wilkerson, 1967) to provide a calibration curve. The curve would be that of the received signal versus the gradient of refractive index averaged over the region approximately between the antennas and the ground level.

The technique of measuring in this way the spatial refractive index gradient and its variation with time--by purposely setting up a nominally grazing propagation path--is more likely to be successful either for relatively flat terrain with sparse vegetation or for over-water paths. For such a propagation path, the computed smooth earth diffraction loss would indicate a variation of attenuation versus gradient, as illustrated in figure 23. In figure 23 we assume a smooth spherical earth and both terminals at a height that would provide a grazing propagation path for a $k = 4/3$ earth. This simple arrangement serves to illustrate the principle involved and the measurement sensitivity that may be expected. The arrangement is also adaptable for diffraction by isolated terrain features (Dougherty and Maloney, 1964; Dougherty and Wilkerson, 1967).

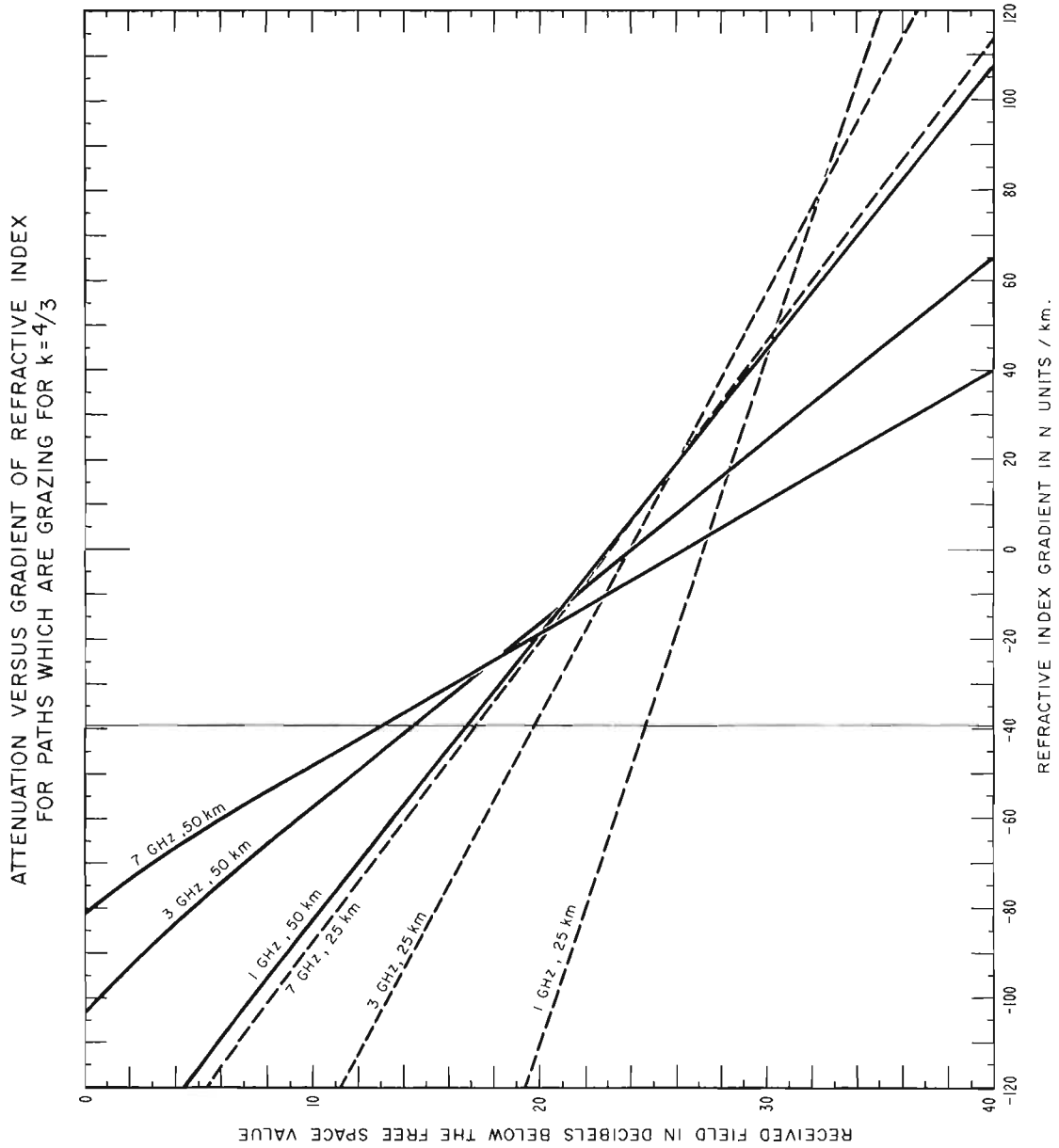
ATTENUATION VERSUS GRADIENT OF REFRACTIVE INDEX
FOR PATHS WHICH ARE GRAZING FOR k=4/3
7 GHz, 50 km
3 GHz, 50 km
1 GHz, 50 km
7 GHz, 25 km
3 GHz, 25 km
1 GHz, 25 km
RECEIVED FIELD IN DECIBELS BELOW THE FREE SPACE VALUE
0
10
20
30
40
120
100
80
60
40
20
0
-20
-40
-60
-80
-100
-120
REFRACTIVE INDEX GRADIENT IN N UNITS / km.

Figure 23

6.2. Diversity Reception as a Measurement Technique

Lewin (1962) employed an interesting technique to check experimentally his diversity reception design procedure. He used a frequency sweeping technique for both the transmitter and the receiver local oscillator in order to obtain an oscilloscopic comparison of the multipath patterns received on two vertically spaced antennas. The transmitter frequency, 4.3. GHz, was swept ± 300 MHz. The local oscillator producing an intermediate frequency of 60 MHz with 10-MHz bandwidth was swept in frequency at a much slower rate. For a synchronization of the oscilloscope sweep and the sweep rate of the transmitter, a time exposure of the oscilloscope presentation of the received signal on one antenna would show a multiple exposure of the IF band pass for which the envelope represents the multipath pattern. This is illustrated schematically in figure 24 (adapted from Lewin, 1962), where the oscilloscope pattern of the received signal (amplitude versus frequency) for the two vertically spaced antennas is displayed in a "push-pull" manner. The sinousoidal envelopes of figure 24 are based on the assumption that the transmitter and oscillator sweep have the same time function.

For multipath due to ground reflections, the nulls may not generally be quite as sharp as indicated in figure 24, because of a less-than-unity specular reflection coefficient and contributions from random nonspecular components. All of the parameters (a, b, α, β, ℓ, L, indicated in fig. 24) are functions of the refractive index gradient averaged over the multipath propagation paths. There are five unknown parameters involved: the magnitude of the reflection coefficient, R; the phase of the reflection coefficient; the effective earth-radius factor, k; and the two antenna heights relative to the equivalent reflection plane, h_1, h_2. At microwave frequencies and for the geometry of the propagation paths of interest, the phase of the reflection coefficient may be closely approximated by π radians for both vertical and horizontal polarization.

A SWEEP FREQUENCY DISPLAY OF DIVERSITY RECEPTION

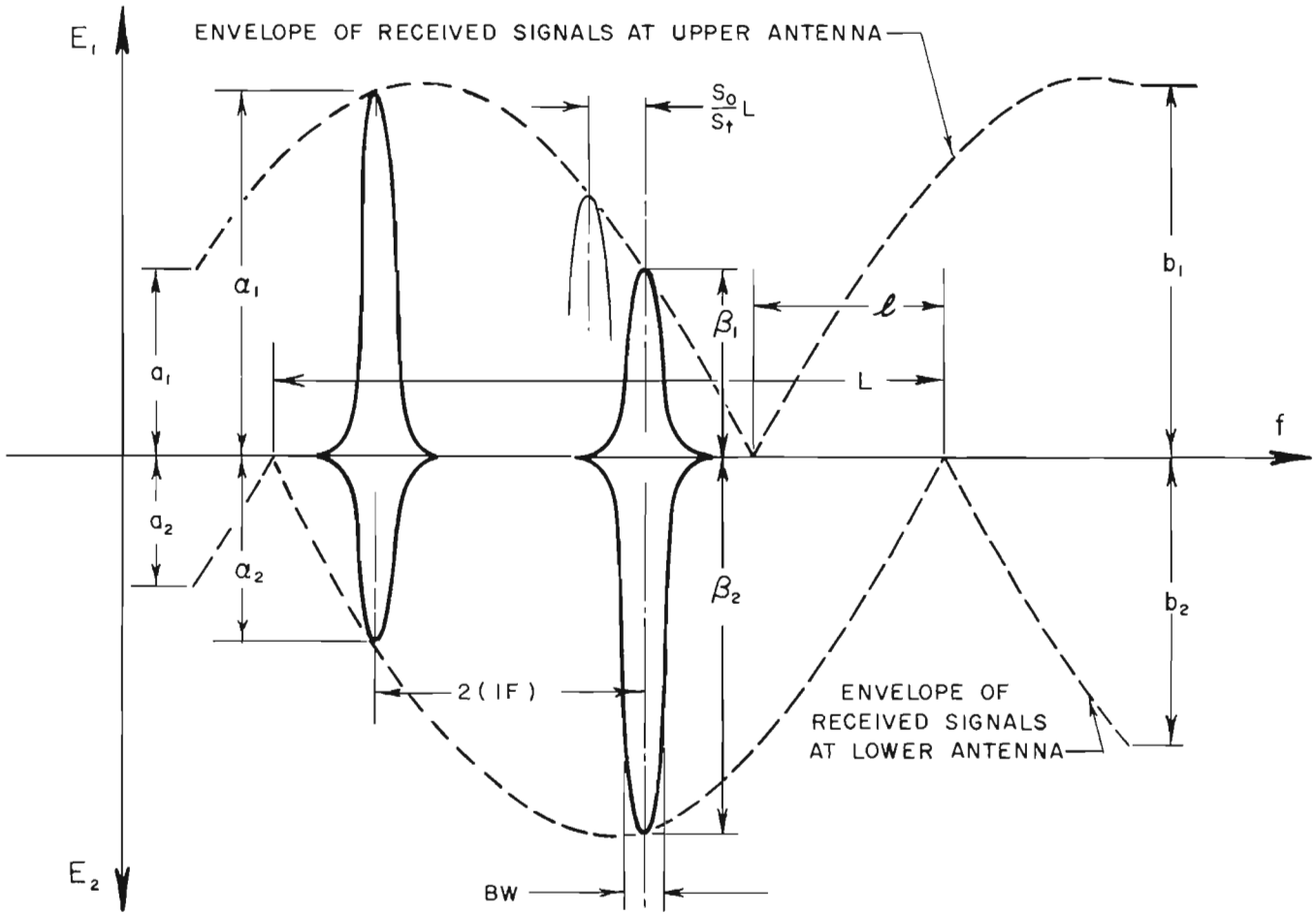

Figure 24

For those propagation paths for which a distinct lobe pattern approximating the one shown in figure 24 is observed, an estimate of R is provided by the peak a_{max} and the null a_{min} amplitudes. That is,

$$R = (r-1)/(r+1) \quad , \tag{20}$$

where $r = a_{max}/a_{min}$. The phase for path length difference may be deduced from figures 24 and 25 and the expressions of section 5 since

$$a_1 = \sin \pi \nu(h_1, k, f+\Delta f) \quad ,$$

$$b_1 = \sin \pi \nu(h_1, k, f-\Delta f) \quad ,$$

$$a_2 = \sin \pi \nu(h_2, k, f+\Delta f) \quad , \text{ and}$$

$$b_2 = \sin \pi \nu(h_2, k, f-\Delta f) \quad , \tag{21}$$

where f is the transmitter oscillator frequency (4.3 GHz) and Δf is the transmitter frequency sweep (300 MHz). The h_1 and h_2 are, of course, the upper and lower antenna heights relative to the reference elevation. The k identifies the effective gradient along the propagation path. Similarly, if we designate as γ the ratio of L to the full horizontal extent of the envelope of figure 24, then we can write

$$f_b - f_a = 2\gamma \Delta f \quad , \tag{22}$$

and k is determined by the condition that $\nu(h_1, k, f_a)$ and $\nu(h_1, k, f_b)$ are both integers that differ by unity. Furthermore,

$$\nu(h_1, k, f_b) = \nu(h_2, k, f_b - \Delta f[\ell/L]) \quad , \tag{23}$$

where ℓ is as defined in figure 24.

The above frequency sweep technique provides a multiplicity of estimates. Much may still be deduced from measurements involving only two transmission frequencies, f_1 and f_2, and two receiving antennas, h_1 and h_2. For example, the direct plus reflected field is given by

$$E_{mn} = 1 - Re^{-j2\pi \nu_{mn}} \quad , \tag{24}$$

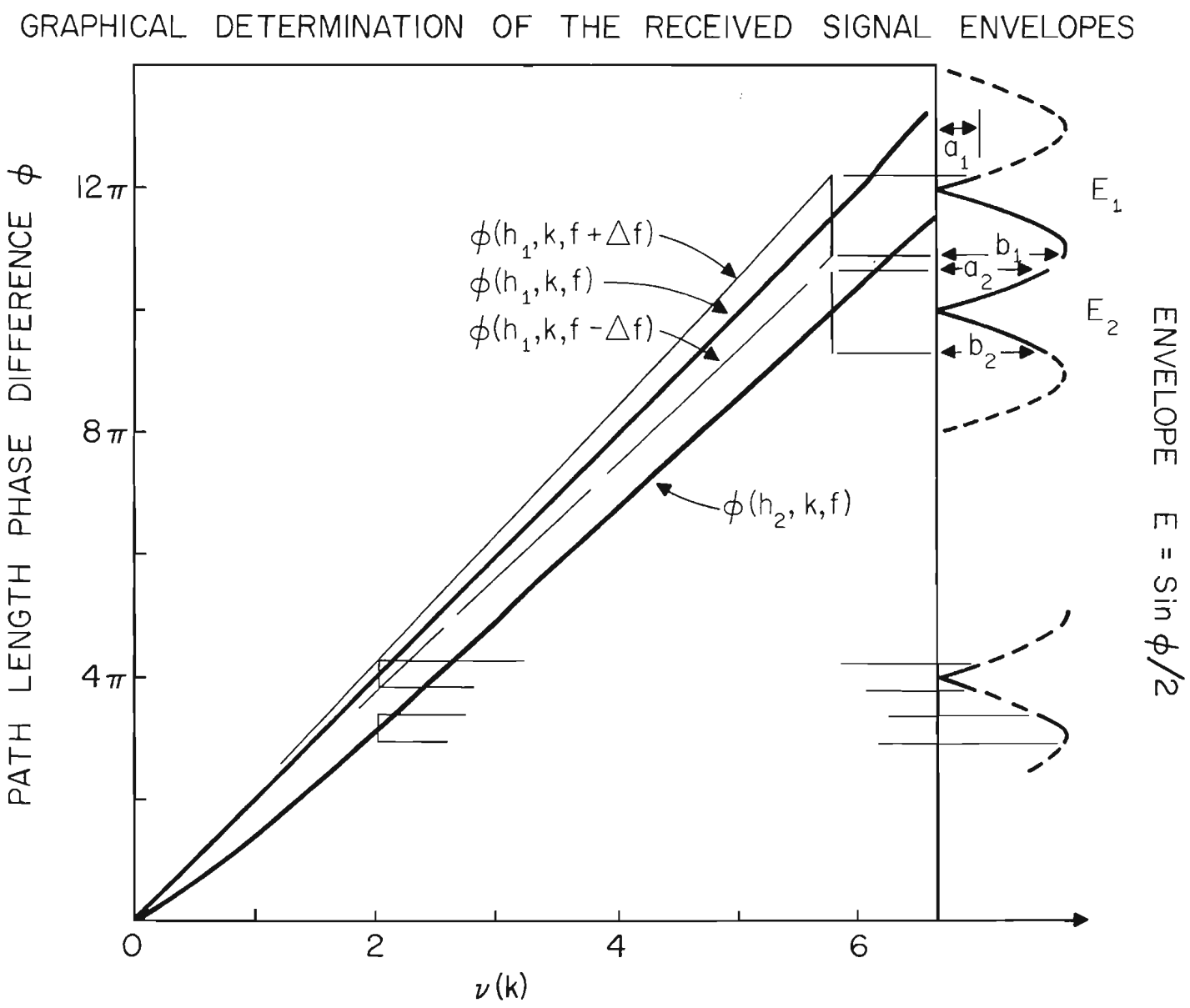
GRAPHICAL DETERMINATION OF THE RECEIVED SIGNAL ENVELOPES
PATH LENGTH PHASE DIFFERENCE φ
12π
8π
4π
0
2
4
6
ν(k)
φ(h1,k,f+Δf)
φ(h1,k,f)
φ(h1,k,f-Δf)
φ(h2, k,f)
a1
b1
a2
b2
E1
E2
ENVELOPE E = Sin φ/2

Figure 25

where the normalized path length difference,

$$\nu_{mn} = \nu(h_m, k, f_n), \quad m = 1, 2; n = 1, 2. \tag{25}$$

Recording of the received signal at two frequencies and two antenna heights gives the four values necessary to deduce the four unknowns R, k, h_1, h_2. The expressions of section 5 permit determination of k. Using the primes to identify antenna heights relative to a reflecting plane, we find

$$\nu_{mn} = \nu(h_m, k, f_n) = 6.673\ 10^{-3}\ \frac{h'_0 h'_m f_n}{d}\ , \tag{26}$$

and Δh is the spacing between the receiving antennas. We can write

$$h'_1 = \Delta h\ \frac{\nu_{1n}/\nu_{2n}}{\nu_{1n}/\nu_{2n} - 1} = \frac{\Delta h\, \nu_{1n}}{\nu_{1n} - \nu_{2n}} \tag{27}$$

$$h'_2 = h'_1 - \Delta h = \frac{\Delta h\, \nu_{2n}}{\nu_{1n} - \nu_{2n}} \tag{28}$$

$$h'_0 = \frac{10^3}{6.673}\ \frac{d\, \nu_{mn}}{h_m f_n}\ . \tag{29}$$

For a terrain profile drawn for the appropriate k value, a straight line drawn in a way to produce the above effective antenna heights should coincide with the terrain at the reflection point. Similarly, reflection attributed to an elevated layer must indicate a reflecting layer consistent with meteorological data. This technique of employing combinations of frequency and space diversity is now being applied, in conjunction with meteorological measurements, to an experimental path in Colorado to verify the effects of the meteorological conditions upon microwave propagation.

7. CONCLUSION

Much is known about the phenomena classed as microwave fading and most of the available information permits classification of the wave propagation mechanisms, supporting meteorological conditions and remedial techniques. Although the information is extensive, there are still many areas that need further investigation. These areas fall naturally into the three problem aspects of microwave fading: prediction, diagnosis, and remedy.

The PREDICTION of fading phenomena is feasible in the sense that the meteorological conditions likely to occur and support microwave fading can often be identified for specific propagation paths. This has yet to be done, however, in a manner that the systems engineer can readily adopt. The problem is to formulate the experience and knowledge of the radio meteorologists in a form that supplements the communication systems engineer's own experience and knowledge. One solution would be a handbook description of microwave fading. This could include diagrams that illustrate the appearance of the recorded signal for particular types of fading, its amplitude distribution, the ray path configuration and the characteristics of the supporting meteorological conditions. As an example, consider the combination of figure 7, 16a, 13, 4, and 3 as a description of multipath fading for the enhancement of ground reflections by antenna decoupling caused by strong superrefractive gradients at night.

The DIAGNOSIS of fading situations would benefit much from the above, but also requires a more detailed description of the fading characteristics. The problem is to distinguish between the fading mechanisms with each category. How does one tell the difference between the multipath signals resulting from ground reflections from those caused by elevated layers? This requires additional data on the

relative amplitudes that may be expected for the components provided by the various types of atmospheric stratification. Also, are there characteristic variations of the meteorological structure with time for the multipath caused by ground reflections and that caused by elevated layers? One would expect so. If there are such characteristic variations, are they sufficiently different to produce different fading rates and fade durations? If so, may they be described quantiatively to serve as distinguishing characteristics of the signal? The problem is similar for power fading. One solution to these problems is the design and implementation of critical experiments.

The choice and design of REMEDIAL techniques are likely to be strongly influenced by advances in prediction and diagnosis. In addition, the effects of the remedial techniques must be better understood. The problem is not simply that of choosing the remedy for a particular fading situation. A knowledge of the remedy limitations is also required. For example, in the design of a diversity system to reduce the effects of multipath caused by ground reflections, what diversity separations will meet that requirement and also be partially effective for multipath caused by elevated layers? Will the choice of separations provide any protection against power fading caused by elevated layers? Fortunately, the design of critical experiments to improve the diagnosis of fading will also meet the need for further investigation of fading remedies.

The above does not pose all of the questions that arise in connection with microwave fading. It does exemplify the many more that will have occurred to the reader who has come this far. This will be particularly true for the reader who has a fading problem! If so, the objective of this report has been achieved: to provide answers to questions previously raised, and to pose new questions.

In addition to the foregoing, there is a broad range of questions associated with modulation system design, antenna design, economic considerations, etc. Although these lie outside the scope of the present report, the subject matter should contribute to the formulation and resolution of these questions. Further progress in understanding fading phenomena will, of necessity, be tied closely to the various experimental investigations carried on, now and in the future, by those organizations supporting, or participating in, the series of experiments recommended by a JTAC subcommittee (1965).

8. ACKNOWLEDGMENT

The author acknowledges the many tangible contributions to this report that resulted from numerous discussions of the various aspects of microwave fading with G. A. Hufford and R. E. McGavin of the ESSA staff. The form of the multipath parameters presented in section 5.1 was developed by Dr. Hufford in an unpublished report, as were the extremely useful nomographs and computational aids upon which figures 21a, 21b, and 21c are based.

9. REFERENCES

Albertson, J. N. (1964), Space diversity on the microwave system of the Southern Pacific Co., Wire and Radio Comm., No. 11, 83-87.

Barsis, A.P., and M.E. Johnson (1961), Prolonged space-wave fadeouts in tropospheric propagation, NBS Tech. Note No. 88 (U.S. Gov't Printing Office, Washington,D.C.).

Barsis, A. P., and M. E. Johnson (1962), Prolonged space-wave fadeouts in tropospheric propagation, J. Res. NBS 66D, (Radio Prop.), No. 2, 681-694.

Bateman, R. (1946), Elimination of interference-type fading at microwave frequencies with spaced antennas. Proc. IRE 34, No. 5, 662-676.

Bean, B. R. (1954), Prolonged space-wave fadeouts at 1046 Mc observed in Cheyenne Mountain propagation program, Proc. IRE 42, No. 5, 848-853.

Bean, B. R. (1964), Tropospheric refraction, Advances in Radio Research, 1, 53-120, ed. J. A. Saxton (Academic Press, London).

Bean, B. R., V. R. Frank,and J. A. Lane (1963), A radiometeorological study, Part II. An analysis of VHF field strength variations and refractive index profiles, J. Res. NBS 67D (Radio Prop.), No. 6, 597-604.

Bean, B. R.,and B. D. Warner (1965), Some radio-physical considerations in studies of the fine scale structure of the atmosphere, Atmospheric Turbulence and Radio Wave Propagation, (Nauka Publishing House, Moscow).

Bean, B. R.,and E. J. Dutton (1966), Radio Meteorology, NBS Monograph 92 (U. S. Gov't Printing Office, Washington, D. C.).

Bean, B. R., B. A. Cahoon, C.A. Samson , and G. D. Thayer (1966), A World Atlas of Atmospheric. Radio Refractivity, ESSA Monograph No. 1 (U. S. Gov't Printing Office, Washington, D. C.) .

Beckmann, P. (1963), Propagation of Ultra-Short Waves (in German) Chap. III, 33-58 (Leipzig).

Beckmann, P. (1962), Statistical distribution of the amplitude and phase of a multiply-scattered field, J. Res. NBS 66D, (Radio Prop.) No. 3, 231-240.

Beckmann, P. and A. Spizzichino (1963). The Scattering of Electromagnetic Waves from Rough Surfaces, (MacMillan Co., N. Y.).

Beckmann, P. (1964), Rayleigh distribution and its generalizations, Radio Sci., J. Res., NBS 68D, No. 9, 927-932.

Born, M. and E. Wolf (1964), Principles of Optics, Chap III, 2nd ed. (Pergamon Press, New York).

Brekhovskikh, L. (1960), Waves in Layered Media (Academic Press, New York).

Bremmer, H. (1949), Terrestrial Radio Waves (Elsevier Publishing Co., New York).

Burns, W. R. (1964), Some statistical parameters related to the Nakagami-Rice probability distribution, Radio Sci. J. Res., NBS 68D, No. 4, 429-434.

Bussey, H. E. (1950), Reflected ray suppression, Proc. IRE 38, No. 12, 1453.

Cabessa, R. (1955), The achievement of reliable radio communication links over maritime paths in Greece (in French), L'Onde Electrique 35, 714-727.

Cahoon, B. A. and L. P. Riggs (1964), Climatology of elevated super-refractive layers arising from atmospheric subsidence, Proc. 1964 World Conference on Meteorology (Am. Met. Soc., Boston).

CCIR Documents of Study Group V, Study Program 57 (V) Doc. V/TP3 Report 237, May 1965.

Dawson, G. (1961), A space aerial diversity reception technique for microwave radio relay systems, Proc. Microwave Seminar, (Tokyo) 1, Doc. No. 4, 86-101.

Doherty, L. H (1952), Geometrical optics and the field at a caustic with applications to radio wave propagation between aircraft, Res. Rept. EE 138 (Cornell Univ., Ithaca, N. Y.).

Dougherty, H. T. (1964), Bibliography of fading on microwave line of sight tropospheric propagation paths and associated subjects, NBS Tech. Note 302 (U.S. Gov't Printing Office, Washington, D.C.).

Dougherty, H. T., and L. J. Maloney (1964), Application of diffraction by convex surfaces to irregular terrain situations, Radio Sci. J. Res. NBS 68D, No. 2, 239-250.

Dougherty, H. T., and R. E. Wilkerson (1967), Determination of antenna height for protection against microwave diffraction fading, Radio Sci. 2 (New Series), No. 161-165.

Dougherty, H. T. (1967), Microwave fading with airborne terminals, ESSA Tech. Rept. IER 58 - ITSA 55 (U.S. Gov't Printing Office, Washington, D. C.).

DuCastel, F., P. Misme, and J. Voge (1960), Sur le rôle des phénomènes de reflexion dans la propagation lointaine des ondes ultracortes, Electromagnetic Wave Propagation, 670-683 (Academic Press, New York).

Dutton, E. J. (1961), On the climatology of ground-based radio ducts and associated fading regions, NBS Tech. Note 96 (U.S. Gov't Printing Office, Washington, D.C.).

Dutton, E. J., and G. D. Thayer (1961), Techniques for computing refraction of radio waves in the troposphere, NBS Tech. Note 97 (U.S. Gov't Printing Office, Washington, D.C.).

Furutsu, K. (1965), On the field strength over a concave spherical earth (To be published).

Hogg, D. C. (1967), Path diversity in propagation of millimeter curves through rain, Trans. IEEE AP-15, No. 3, 410-415.

Hoyt, R. W. (1947), Probability functions for the modulus and angle of the normal complex variety, Bell System Tech. J. 26 , 318-359.

Hufford, G. A. (1952), An integral equation approach to the problem of wave propagation over an irregular surface, Quart. Appl. Math. 9, No. 4, 391-404.

Hufford, G. A (1968), On the concept of an effective earth's radius (Submitted to Radio Science for publication).

Hunter, I. (1964), Attenuation of microwaves in the troposphere, Marconi Rev. 27, No. 154, 122-142.

Ikegami, F. (1964), Radiometeorological effects in propagation over the sea and islands. Rev. Tokyo Elec. Comm. Lab. NTT 12, 5-6, 312-324.

JTAC (The Joint Technical Advisory Committee, IEEE-EIA) (1965) Microwave Radio Relay System Reliability, Report to the FCC, 23, March.

Katzin, M. R., W. Bachman, and W. Binnian (1947), Three and nine centimeter propagation in low ocean ducts, Proc. IRE 35, No. 9, 891-905.

Kawazu, S., S. Koto, and K. Morita (1959), Over-sea propagation of microwave and anti-reflected-wave antenna, Reports of ECL, (Japan) 7, 171-191.

Klein, W., and L. J. Libois (1953), Communication experiment with radio beams on a long line-of-sight path between France and Switzerland (in French), L'Onde Electrique 33, 665-677.

Kuhn, V. (1967), Propagation measurements at 8.1 GHz on a line-of-sight path (in German), Tech. Mitt. RFZ 11, No. 2, 65-70.

Lewin, L. (1962), Diversity reception and automatic phase correction, Proc. IEE, Part B, 109, 295-304.

Magnuski, H. (1956), An explanation of microwave fading and its correction by frequency diversity, presented at the AIEE, Winter General Meeting in N. Y., 56-376.

Matsuo, S., S. Ugai, K. Kakito, F. Ikegami, and Y. Kono (1953), Microwave fading, Reports of ECL (Japan) 1, No. 3, 38-47.

Medhurst, R. G. (1965), Rainfall attenuation of centimeter waves: comparison of theory and experiment, Trans. IEEE AP-13, No. 4, 550-564.

Millington, G. (1957), The concept of the constant radius of the earth in tropospheric propagation, Marconi Rev. 20, 79-93.

Millington, G. (1946), Curved earth geometrical optics, Marconi Rev. 9, No. 1, 1-12.

Misme, P. (1957), The influence of frontal discontinuities on the propagation of decimeter and centimeter waves (in French), Ann. Telecomm. 12, 189-194.

Murray, J. W., and H. M. Flager (1965), Improving microwave system reliability, First IEEE Annual Comm. Convention Conference Record, Boulder, Colo., 245-248.

Nakagami, M. (1943), Statistical characteristics of short wave fading, J. Inst. Elec. Comm. Eng. Japan 239, 145.

Nakagami, M. (1964), On the intensity distributions and its application to signal statistics, Radio Sci. J. Res. NBS 68D, No. 9, 995-1003.

Nicolis, J. S. (1966), Fading statistics on a 212-km line-of-sight overwater radio path A 1760 MHz, ESSA Tech. Rept. IER 14-ITSA 14 (U.S. Gov't Printing Office, Washington, D. C.).

Nicolis, J. S. (1967), Some aspects of the deep and/or rapid fading phenomena in strictly line-of-sight VHF/SHF propagation, ESSA Tech. Rept. IER 23-ITSA 23 (U.S. Gov't Printing Office, Washington, D.C.).

Norton, K. A., L.E. Vogler, W.V. Mansfield, and P.J. Short (1955), The probability distribution of the amplitude of a constant vector plus a Rayleigh-distributed vector, Proc. IRE 43, No. 10, 1354-1361.

Norton, K. A., G. A. Hufford, H. T. Dougherty, and R. E. Wilkerson (1965), Diversity design for within-the-horizon radio relay systems. (An unpublished report.)

Preikschat, F. K. (1964), Screening fences for ground reflection reduction, Microwave Journal 7, No. 8, 46-50.

Quarta, P. (1964), Aleuni aspetti della propagazione della microonde su mare, Alta Frequenza 33, No. 1, 22-30.

Quarta, P. (1966), Propagation tests on an oversea path (Mt. Verrugoli-Mt. Portofino), Alta Frequenza, 35, No. 5, 364-369.

Rice, P. L., A.G. Longley, K.A. Norton, and A.P. Barsis (1966), Transmission loss predictions for tropospheric communication circuits Vols. I, II, NBS Tech. Note 101, (U.S. Gov't Printing Office, Washington, D. C.).

Rice, S. O. (1944; 1945), Mathematical analysis of random noise, Bell System Tech. J. 23, 282-332; 24, 46-156.

Ryde, J.W. and D. Ryde (1945), Attenuation of centimeter waves by rain, hail, fog, and clouds (Gen. Elec., Wembly, England).

Sharpless, W. M. (1946), Measurement of the angle of arrival of microwaves, Proc. IRE 34, No. 11, 837-845.

Schelleng, J. C., C. R. Burrows, and E. B. Ferrell (1933), Ultra-short wave propagation, Proc. IRE 21, No. 3, 427-463.

Troitskii, V. N. (1960), The propagation of centimeter waves on long-distance mountain routes, Radio Eng. Electron. 5, 61-69.

Ugai, S., S. Aoyagi, and S. Nakahara (1963), Microwave transmission across a mountain by using diffractor gratings (in Japanese), J. Inst. Elec. Comm. Eng. (Japan) 46, 653-661.

Vogler, L. E. (1964), Calculation of ground-wave attenuation in far diffraction region , Radio Sci. J. Res. NBS 68D , No. 7, 819-826.

Wait, J. R. (1962), Electromagnetic Waves in Stratified Media, (Pergamon Press, Oxford .).

Wait, J. R. (1964), A note on VLF reflection from a tropospheric layer, Radio Sci. J. Res. NBS 68D, No. 7, 847-848.

Wilkerson, R. E. (1962), Defocusing of radio rays by the troposphere, J. Res. NBS 66D (Radio Prop.), No. 4, 479-485.

10. APPENDIX

The Angle-of-Arrival and the Earth-Radius Factor

The curvature of a radio ray path relative to the earth curvature has been given by 1/k in (1) of the text. Figure 26 illustrates the departure of such a ray path from its initial direction; this is given by

$$\frac{x^2}{2r_0} - \frac{x^2}{2kr_0} \quad , \tag{A-1}$$

at a distance x from the launch point.

The departure of this ray path from its cord between end points is therefore

$$\delta = \left[\frac{x}{d}\left(\frac{d^2}{2kr_0}\right) - \frac{x^2}{2kr_0}\right](k-1) = \frac{x(d-x)}{2kr_0}(k-1) \ , \tag{A-2}$$

in terms of the rectangular coordinates, x and y, with origin at some reference elevation on a spherical earth. The transmitting antenna at elevation H_1 (relative to the same reference) is at y = 0. The receiving antenna is at elevation H_2, x = d. Due to the earth's curvature, the receiving antenna's location is

$$y_2 = H_2 - \frac{d^2}{2r_0} \quad , \tag{A-3}$$

and the chord of the ray path is therefore

$$y(k = 1, x) = H_1 + \frac{x}{d}\left[H_2 - H_1 - \frac{d^2}{2r_0}\right] \ . \tag{A-4}$$

Combining (A-2) and (A-4), the equation of the ray path is

SCHEMATIC DIAGRAM FOR THE
DERIVATION OF THE ANGLE OF ARRIVAL

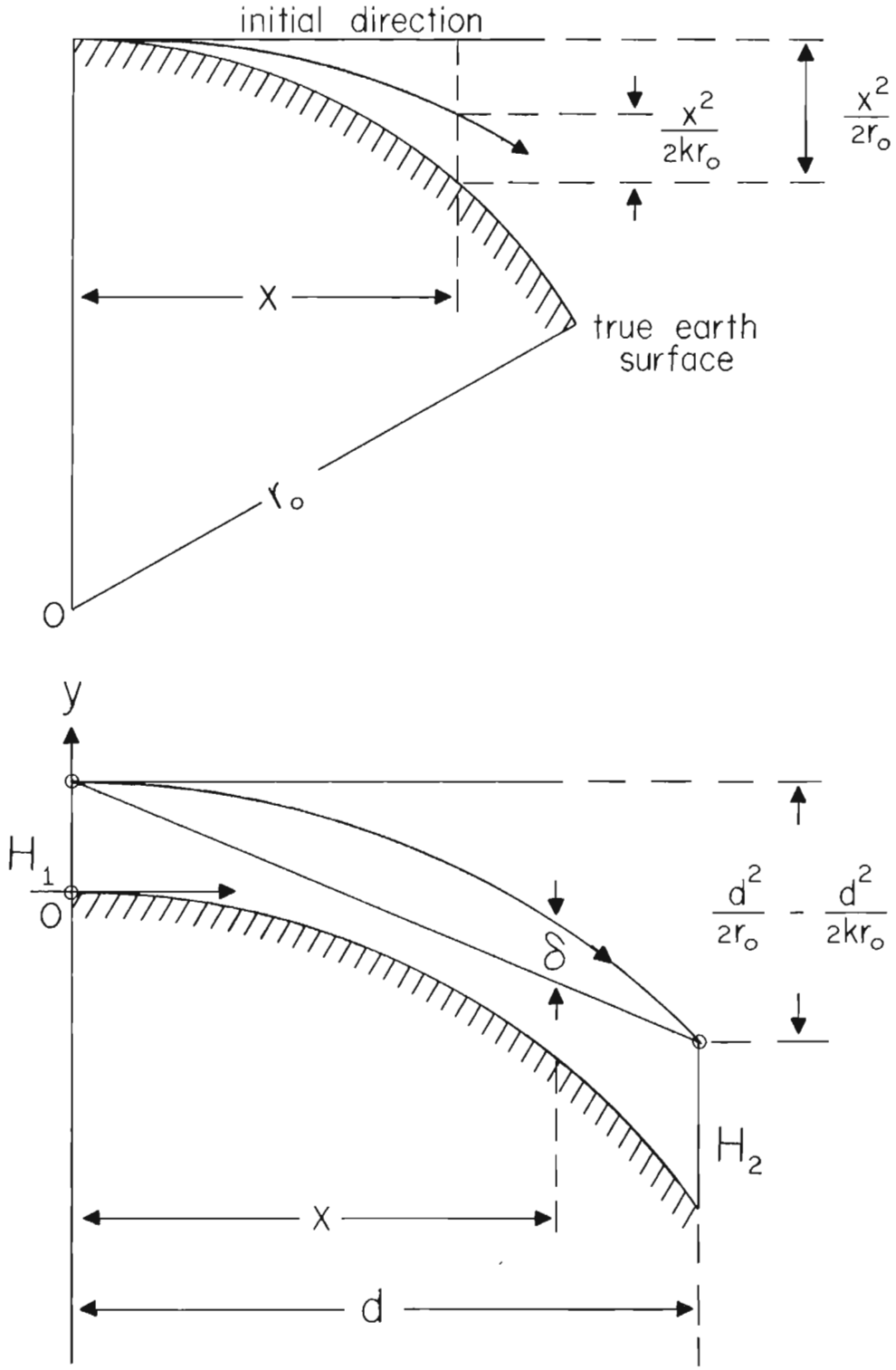

Figure A-1

$$y(k, x) = H_1 + \frac{x}{d}\left[H_2 - H_1\right] - \frac{xd}{2kr_0} - \frac{x^2}{2kr_0} \quad . \qquad \text{(A-5)}$$

Evaluating the first derivative with respect to x of (A-5) at x = 0, we obtain

$$y'(k, 0) = \frac{H_2 - H_1}{d} - \frac{d}{2kr_0} \quad . \qquad \text{(A-6)}$$

The first term is a measure, $\tan \theta_1(\infty)$, of the initial direction of the ray for a flat earth and so

$$\tan \theta_1(k) - \tan \theta_1(\infty) = - \frac{d}{2kr_0} \quad . \qquad \text{(A-7)}$$

Incorporating $r_0 = 6370$ km, we find

$$\tan \theta_1(k) - \tan \theta_1(\infty) \approx -0.0785\ d/k \text{ mrad.} \qquad \text{(A-8)}$$

GPO 842-719